

*Pacific
Journal of
Mathematics*

SEMISIMPLE TUNNELS

SANGBUM CHO AND DARRYL McCULLOUGH

SEMISIMPLE TUNNELS

SANGBUM CHO AND DARRYL MCCULLOUGH

A knot in S^3 in genus-1 1-bridge position (called a $(1, 1)$ -position) can be described by an element of the braid group of two points in the torus. Our main results tell how to translate between a braid group element and the sequence of slope invariants of the upper and lower tunnels of the $(1, 1)$ -position. After using them to verify previous calculations of the slope invariants for all tunnels of 2-bridge knots and $(1, 1)$ -tunnels of torus knots, we obtain characterizations of the slope sequences of tunnels of 2-bridge knots, and of a class of tunnels we call toroidal. The main results lead to a general algorithm to calculate the slope invariants of the upper and lower tunnels from a braid description. The algorithm has been implemented as software, and we give some sample computations.

Introduction

Genus-2 Heegaard splittings of the exteriors of knots in S^3 have been a topic of considerable interest and recent progress. Usually these are discussed in the language of tunnels, which we will use from now on. In particular, the term tunnel will mean a tunnel of a tunnel number 1 knot in S^3 .

A rich source of examples of tunnels are the upper and lower tunnels associated to a knot positioned with bridge number 1 with respect to a standard torus in S^3 . Traditionally this is called a $(1, 1)$ -position of the knot, and the associated tunnels are called $(1, 1)$ -tunnels.

In [Cho and McCullough 2009a], we laid out a theory of tunnels based on the disk complex of the genus-2 handlebody. It provides a unique construction of each knot tunnel by a sequence of “cabling” constructions, each determined by a rational “slope” invariant (the slope invariant of the first cabling is only defined in \mathbb{Q}/\mathbb{Z}). There is a second invariant, a binary sequence, which is trivial for $(1, 1)$ -tunnels. Thus the sequence of slope invariants is a complete invariant for a $(1, 1)$ -tunnel.

McCullough was supported in part by NSF grant DMS-0802424. Cho is supported by Basic Science Research Program through the National Research Foundation of Korea (NRF) funded by the Ministry of Education, Science and Technology (2012006520).

MSC2010: 57M25.

Keywords: knot, tunnel, $(1, 1)$, braid, torus, slope, invariant, cabling, semisimple, 2-bridge, toroidal, algorithm.

Naturally it is not very easy to calculate a complete invariant, but the invariants are known for all the tunnels of 2-bridge knots [Cho and McCullough 2009a, Section 15] and torus knots [Cho and McCullough 2009b]. K. Ishihara [2011] has given a computational algorithm which is effective for some examples.

There is a simple description of a $(1, 1)$ -position in terms of a braid of two points in a standard torus T in S^3 : Regard the braid as two arcs in $T \times I \subset S^3$, connect the top two points with a small trivial arc in the “upper” solid torus, and similarly for the bottom two points in the “lower” solid torus. Many different braids can give equivalent $(1, 1)$ -positions. Some of this ambiguity is resolved by using the quotient of the braid group by its center, which we call the reduced braid group. A braid that produces the $(1, 1)$ -position is called a braid description of it. In Section 1, we will examine braid descriptions and the reduced braid group, before detailing in Section 2 the first of several “maneuvers” involving braids and $(1, 1)$ -positions. Sections 3–6 contain a review of our general theory of tunnels, focusing on the parts needed for this paper.

Our main results are Theorems 8.1 and 9.3, which allow one to pass back and forth between a braid description of a $(1, 1)$ -position and the cabling slope sequence of its upper (or its lower) tunnel. This has several applications. In Example 9.4, we show how to find a braid description and use it to calculate the slope invariants for a more-or-less random example, the knot and tunnel drawn in Figure 10 of [Cho and McCullough 2009a]. In Section 10 we use braid descriptions for the $(1, 1)$ -positions of all 2-bridge knots to recover the general calculation of slope invariants obtained in the same work. We also give a precise characterization of the slope sequences that arise from tunnels of 2-bridge knots. In Section 11, we use braid descriptions for the $(1, 1)$ -positions of torus knots (each has a unique $(1, 1)$ -position) to recover the slope invariants for their upper and lower tunnels, first found in [Cho and McCullough 2009b].

A more theoretical application is given in Section 12, where we show that a certain property of the sequence of slope invariants corresponds to a $(1, 1)$ -position in $T \times I$ with no critical points in either of the S^1 -directions. We call such positions *toroidal* positions. Among the 2-bridge knots, only the $(2n + 1, \pm 2)$ -torus knots admit a toroidal position.

Our final applications make the procedure of passing between braid descriptions and slope invariants completely algorithmic. Passing from the sequence of slope invariants to a braid description is rather easy, as seen in Section 13. The other direction, detailed in Section 14, is more difficult, since anomalous infinite-slope cablings can arise (technically speaking, these are not even “cablings”) when the braid word is put into its standard form, and one must manipulate the word to eliminate these. Both of the algorithms, as well as the general slope calculations for 2-bridge knot tunnels and $(1, 1)$ -tunnels of torus knots, are very effective and have

been implemented in Python; the software is available in the [Electronic Supplement](#) or at [\[Cho and McCullough 2010b\]](#). (See also [www.math.ou.edu/~dmccullough](#) for other software that finds the invariants for the “middle” tunnels of torus knots.) Sample calculations are given in [Section 15](#).

1. Braid descriptions of (1, 1)-positions

In this section, we recall the 2-braid group on the torus, and its quotient by its center. The latter, which we call the *reduced braid group* \mathcal{B} , or just the *braid group*, will play a central role in our work. We will also see how an element $\omega \in \mathcal{B}$ describes a knot $K(\omega)$, and moreover a (1, 1)-position of that knot.

Let T be a standard torus in S^3 , bounding a solid torus $W \subset S^3$. In our figures, W usually lies above T . Denoting the unit interval $[0, 1]$ by I , fix a collar $T \times I \subset S^3 - W$ with $T = T \times \{0\}$, and denote by V the solid torus $S^3 - (W \cup T \times I)$.

Fix a point $b \in T$, which we will refer to as the *black point*. Fix standard meridian and longitude curves m and ℓ in T such that

- (i) $m \cap \ell = b$,
- (ii) m bounds a disk in $V \cup T \times I$, and
- (iii) ℓ bounds a disk in W .

Choose a point w in T that is not in $m \cup \ell$. We will refer to w as the *white point*.

A braid can be described geometrically as a pair of disjoint arcs properly embedded in $T \times I$ such that each endpoint of the arcs is one of $b \times \{0\}$, $b \times \{1\}$, $w \times \{0\}$, or $w \times \{1\}$, and each of the arcs meets each $T \times \{s\}$ transversely in a single point. There is an obvious multiplication operation on the collection of such pairs defined by “stacking” two pairs.

Two such pairs are equivalent if there is an isotopy J_t of $T \times I$ such that

- (i) $J_0 = id_{T \times I}$,
- (ii) $J_t|_{T \times \partial I} = id_{T \times \partial I}$ for $t \in [0, 1]$,
- (iii) $J_t(T \times \{s\}) = T \times \{s\}$ for $s \in [0, 1]$ and $t \in [0, 1]$, and
- (iv) J_1 sends one pair to the other pair.

The multiplication operation induces a group structure on the set of equivalence classes, producing $\mathcal{B}_2(T)$, the classical braid group of two points in the torus.

A presentation of $\mathcal{B}_2(T)$ is given in [\[Birman 1969; Takebayashi 2006\]](#). We rewrite it as

$$\langle \delta_m, \delta_\ell, \sigma \mid \delta_m \sigma \delta_m \sigma = \sigma \delta_m \sigma \delta_m, \delta_\ell \sigma \delta_\ell \sigma = \sigma \delta_\ell \sigma \delta_\ell, \\ \delta_m^{-1} \delta_\ell \delta_m \delta_\ell^{-1} = \sigma^2, \sigma \delta_\ell \sigma \delta_m = \delta_m \sigma \delta_\ell \sigma^{-1} \rangle.$$

In the notation of [\[Takebayashi 2006\]](#), $\delta_m = y_1$, $\delta_\ell = x_1^{-1}$, and $\sigma = s_1$.

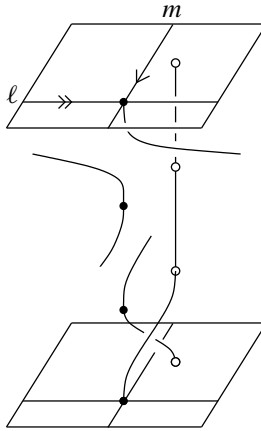


Figure 1. An imbedding that represents the element $\delta_\ell \delta_m \sigma$ in $\mathcal{B}_2(T)$. We read braids from the top down, so in this picture, the solid torus W lies above the upper copy of the torus, which is $T = T \times \{0\}$.

As seen in [Figure 1](#), representatives of δ_m and δ_ℓ slide the black point around m and ℓ respectively, while keeping the white point fixed. A representative of σ produces a half-twist of the two strands, as shown.

Now we weaken condition (ii) in the definition of equivalence of braids to

$$(ii') \quad J_1|_{T \times \partial I} = id_{T \times \partial I}.$$

That is, we do not require that each J_t be the identity on $T \times \partial I$ for $t \in (0, 1)$. We call the new equivalence classes of the pairs of arcs under this condition *reduced braids*, and the group of all reduced braids is the *reduced braid group*, denoted by \mathcal{B} .

The fundamental group $\pi_1(T) = \mathbb{Z} \times \mathbb{Z}$ can be regarded as a subgroup of $\mathcal{B}_2(T)$, as the subgroup generated by $\delta_\ell \sigma \delta_\ell \sigma$ and $\delta_m \sigma \delta_m \sigma$. [Figure 2](#) illustrates a pair of

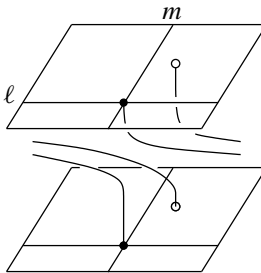


Figure 2. A braid that represents $\delta_\ell \sigma \delta_\ell \sigma$. A similar pair, winding in the m -direction, represents $\delta_m \sigma \delta_m \sigma$.

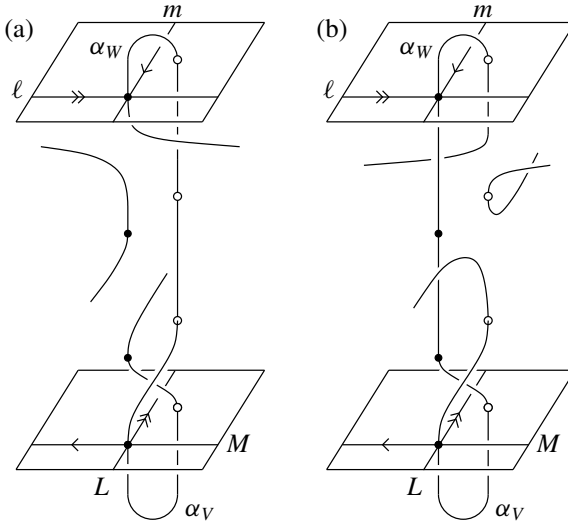


Figure 3. Two imbeddings representing the element $\delta_\ell \delta_m \sigma$ in \mathcal{B} . Also shown are the meridian M and longitude L for the reverse braid $\sigma \delta_L \delta_M$, and the trivial arcs α_W and α_V added to form the knot $K(\delta_\ell \delta_m \sigma)$. It is the trivial knot.

arcs representing $\delta_\ell \sigma \delta_\ell \sigma$ in $\mathcal{B}_2(T)$. Using the presentation of $\mathcal{B}_2(T)$, one can verify that $\pi_1(T)$ is central in \mathcal{B} .

Weakening condition (ii) to (ii') has the effect of making the braids $\delta_\ell \sigma \delta_\ell \sigma$ and $\delta_m \sigma \delta_m \sigma$ trivial. On the other hand, the additional isotopies allowed by condition (ii') are just products of the isotopies that move those two braids to the trivial braid (or the reverses of these isotopies). Thus (ii') has the effect of adding the two relations $\delta_m \sigma \delta_m \sigma$ and $\delta_\ell \sigma \delta_\ell \sigma$ to the above presentation of $\mathcal{B}_2(T)$, giving the following proposition.

Proposition 1.1. *The reduced braid group \mathcal{B} has the presentation*

$$\langle \delta_m, \delta_\ell, \sigma \mid (\delta_m \sigma)^2 = (\delta_\ell \sigma)^2 = 1, \delta_m^{-1} \delta_\ell \delta_m \delta_\ell^{-1} = \sigma^2 \rangle.$$

As shown in Figure 3(b), in \mathcal{B} there are other representatives of δ_m and δ_ℓ that slide the white point backwards along loops parallel to m and ℓ respectively. An isotopy that moves $b \times \{0\}$ around the loop ℓ changes the first representative of δ_ℓ , that moves the black point strand, to the second, that moves the white point strand in the other direction. Similarly, an isotopy that moves $b \times \{0\}$ around m changes the representative of δ_m that moves the black strand to one that moves the white strand in the other direction. These correspond to the facts that $\sigma^{-1} \delta_\ell^{-1} \sigma^{-1} = \delta_\ell$ and similarly for δ_m .

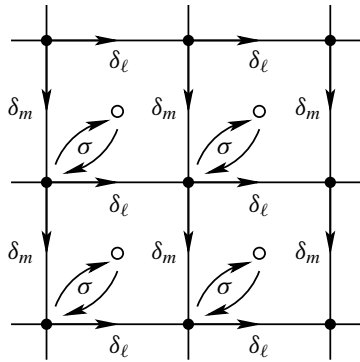


Figure 4. The universal cover of T , illustrating the relations in \mathcal{B} .

A nice way to understand the relations in \mathcal{B} is to consider the picture of the universal cover of T shown in Figure 4. In this picture, δ_ℓ slides the black points one unit to the right, δ_m slides the black points one unit downward, and σ interchanges black and white points as indicated. The product $\sigma\delta_\ell\sigma$ slides the white points one unit to the right, so the effect of $\delta_\ell\sigma\delta_\ell\sigma$ is to slide both black and white one unit to the right. The relation $\delta_m\sigma\delta_m\sigma$ is similar, while the word $\delta_m^{-1}\delta_\ell\delta_m\delta_\ell^{-1}$ corresponds to a braid for which the white points are fixed and the black points travel clockwise around the squares in Figure 4, starting from the lower left-hand corner, which is the effect of σ^2 .

Since we will have no further use for $\mathcal{B}_2(T)$, it is safe just to call \mathcal{B} *the braid group*, and its elements *braids*.

Figure 3 also illustrates the *reverse braid*, which is obtained if one views the picture from below. The meridian and longitude M and L seen from below are analogous to the meridian m and longitude ℓ seen from above. Note that they are interchanged, so that δ_m seen from below is δ_L and δ_ℓ seen from below is δ_M . Although both have the reversed orientation, a braid δ_m or δ_ℓ seen from below has the point moving in reversed time, so δ_m becomes δ_L and δ_ℓ becomes δ_M . On the other hand, σ seen from below still looks like σ . Thus the reverse braid has δ_m replaced by δ_L and δ_ℓ replaced by δ_M , with σ unchanged, and the order of the letters reversed.

Figure 3 also illustrates the *knot described by the braid* ω . One simply attaches the two standard arcs α_V and α_W at the bottom and top. In Figure 3, α_V and α_W are obtained from arcs $\alpha \times \{1\}$ and $\alpha \times \{0\}$ respectively, pushing the former slightly into V and the latter into W , where α is a fixed arc in T connecting b and w , and meeting $m \cup \ell$ only in b . There are four isotopy classes of such arcs, and we select α to lie in the isotopy class that at b leaves m in the direction of the positive orientation on ℓ (using the orientation shown in of Figure 3) and leaves ℓ in the

direction of the negative orientation on m . The lifts of α to the universal covering space of T shown in Figure 4 leave the preimages of b from the lower-left hand corner of each square.

The resulting knot $K(\omega)$ is well-defined, indeed equivalent reduced braids describe knots that are in $(1, 1)$ -position with respect to T and are $(1, 1)$ -isotopic (that is, isotopic by an isotopy of S^3 preserving T at all times). The notation $K(\omega)$ implicitly includes this well-defined $(1, 1)$ -position. We say that $K(\omega)$ is *in braid position*, and that the element ω is a *braid description* of the knot and its $(1, 1)$ -position (with respect to the fixed arc α). A braid and its reverse braid describe isotopic knots, but the two $(1, 1)$ -positions have upper and lower tunnels interchanged.

Observe that $K(\omega)$ and $K(\omega\delta_m)$ are $(1, 1)$ -isotopic, by an isotopy that pushes $K(\omega)$ across the core circle of the solid torus V . Similarly, $K(\omega)$ is $(1, 1)$ -isotopic to $K(\delta_\ell\omega)$, and $K(\omega)$ to both $K(\omega\sigma)$ and $K(\sigma\omega)$. In general, if $W_0(\delta_\ell, \sigma)$ is a word in the letters δ_ℓ and σ , and $W_1(\delta_m, \sigma)$ is a word in δ_m and σ , then

$$K(W_0(\delta_\ell, \sigma)\omega W_1(\delta_m, \sigma)) \quad \text{and} \quad K(\omega)$$

are $(1, 1)$ -isotopic. For example, the knot $K(\delta_\ell\delta_m\sigma)$ in Figure 3 is $(1, 1)$ -isotopic to $K(1)$, hence is trivial.

Notation 1.2. Let $\langle \delta_\ell, \sigma \rangle$ denote the subgroup of \mathcal{B} generated by δ_ℓ and σ , and similarly for $\langle \delta_m, \sigma \rangle$. We will write $\omega_1 \sim \omega_2$ to mean that ω_1 and ω_2 represent the same double coset of the form $\langle \delta_\ell, \sigma \rangle \omega_1 \langle \delta_m, \sigma \rangle$, and consequently are braid descriptions of the same $(1, 1)$ -position.

2. Tunnels in standard position

In this section, we will introduce a basic maneuver. Figure 5(a) shows the torus $T = T \times \{0\}$, the portion of a $(1, 1)$ -knot that lies in W , and a tunnel arc for the

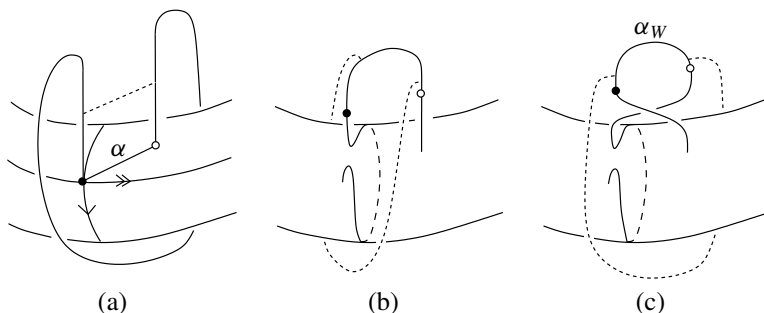


Figure 5. Introduction of an initial $\sigma^{-1}\delta_m^{-1}$ in order to reposition a tunnel into standard position.

“upper” $(1,1)$ -tunnel of the knot. The segment on T connecting black and white vertices is the fixed arc α used to define the $(1, 1)$ -knot from a braid description as in [Section 1](#). The knot is not in braid position, because it does not meet W in an arc parallel to α . There is an isotopy of the knot, preserving $(1, 1)$ -position, that changes the placement in [Figure 5\(a\)](#) to the one in [Figure 5\(b\)](#). The arc of the knot in W moves to a different arc, and a braid letter δ_m^{-1} appears just inside the solid torus. The tunnel arc is stretched out to wind around the core of W . A further $(1, 1)$ -isotopy changes [Figure 5\(b\)](#) to [Figure 5\(c\)](#), introducing another braid letter σ^{-1} . If we push the knot down into $T \times I$ until its intersection with W is parallel to α (or equivalently enlarge $T \times I$ to include the portion of the knot that lies below the black and white points), then the knot is now in braid position (assuming that its original intersection with $V \cup T \times I$ is consistent with braid position).

When the upper tunnel and the portion of K in W consist of a tunnel arc and a trivial arc as in the portion above the black and white points in [Figure 5\(c\)](#), we say that K and the upper tunnel (arc) are in *standard position*. Thus the effect of the maneuver just described is to move a tunnel arc and K that appear as in [Figure 5\(a\)](#) so that K and the tunnel are in standard position, while changing the braid represented by the portion of K in $T \times I$ by premultiplication by $\sigma^{-1}\delta_m^{-1}$. Since $\sigma^{-1}\delta_m^{-1} = (\delta_m\sigma)^{-1} = \delta_m\sigma$ in \mathcal{B} , this is equivalent to premultiplication by $\delta_m\sigma$.

3. Tunnels as disks

Our previous articles [[Cho and McCullough 2009a](#); [2009b](#); [2010a](#); [2011](#)] give the details of our general theory of knot tunnels. Of these, [[2009a](#)] is the most complete, while of the shorter summaries in the other papers, the material in [[2009b](#)] is the closest to our present needs. For convenience of the reader, we will provide in this and the next three sections a review adapted to our work here. It also establishes notation that is used in the rest of the paper.

This section gives a brief overview of the theory in [[Cho and McCullough 2009a](#)]. Fix a “standard” genus-2 unknotted handlebody H in S^3 . Regard a tunnel of K as a 1-handle attached to a neighborhood of K to obtain an unknotted genus-2 handlebody. Moving this handlebody to H by an isotopy of S^3 , a cocore disk for the 1-handle moves to a nonseparating disk in H . The indeterminacy due to the choice of isotopy is exactly the Goeritz group, which is the group of path components of the space of orientation-preserving homeomorphisms of S^3 that take H onto H . Consequently, the collection of all tunnels of all tunnel number 1 knots, up to orientation-preserving homeomorphism, corresponds to the orbits of nonseparating disks in H under the action of the Goeritz group. Indeed, it is convenient for us to *define* a tunnel to be an orbit of nonseparating disks in H under the action of the Goeritz group.

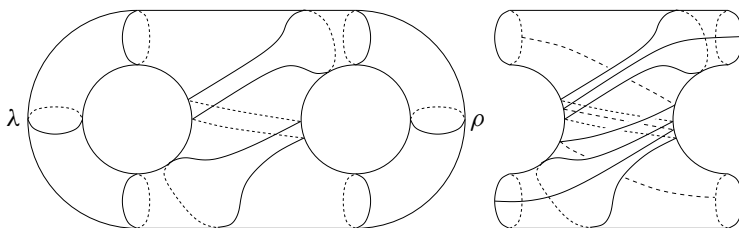


Figure 6. A slope disk of $\{\lambda, \rho\}$, and a pair of its cabling arcs contained in B .

Work of Scharlemann [2004], Akbas [2008], and Cho [2008] gives a very good understanding of the way that the Goeritz group acts on the disks in H . As detailed in [Cho and McCullough 2009a], the orbits (tunnels) can be arranged in a treelike structure which encodes much of the topological structure of tunnel number 1 knots and their tunnels.

When a nonseparating disk $\tau \subset H$ is regarded as a representative of a tunnel, or simply a tunnel itself, the corresponding knot is a core circle of the solid torus that results from cutting H along τ . This knot is denoted by K_τ . For example, in the handlebody shown in Figure 6, a core circle of the solid torus cut off by the middle disk is a trefoil knot.

A disk τ in H is called *primitive* if there is a disk τ' in $\overline{S^3 - H}$ such that $\partial\tau$ and $\partial\tau'$ cross in one point in ∂H . Equivalently, K_τ is the trivial knot in S^3 . All primitive disks are equivalent under the action of the Goeritz group. This equivalence class is the unique tunnel of the trivial knot.

A *primitive pair* is an isotopy class of two disjoint nonisotopic primitive disks in H . A *primitive triple* is defined similarly. All primitive pairs are equivalent under the Goeritz group, as are all primitive triples.

It is important to understand that a triple of nonseparating disks in H corresponds to an isotopy class of θ -curves in H , specifically, the θ -curve whose arcs are “dual” to the three disks — each arc cuts across exactly one of the three disks once, each disk meets exactly one of the three arcs, and each of the balls obtained by cutting H along the union of the three disks deformation retracts to the portion of the θ -curve that it contains. This θ -curve is “unknotted” in S^3 , that is, the closure of the complement of a regular neighborhood is a genus-2 handlebody. Thus an orbit of such triples under the Goeritz group corresponds to an isotopy class in S^3 of unknotted θ -curves.

4. Slope disks and cabling arcs

This section gives the definitions needed for computing the slope invariants that will be discussed in Section 5. Fix a pair of disjoint nonseparating disks λ and ρ

(for “left” and “right”) in the standard unknotted handlebody H in S^3 , as shown abstractly in Figure 6. The pair $\{\lambda, \rho\}$ is arbitrary, so in the true picture in H in S^3 , they will typically look a great deal more complicated than the pair shown in Figure 6. Let N be a regular neighborhood of $\lambda \cup \rho$ and let B be the closure of $H - N$. The frontier of B in H consists of four disks which appear vertical in Figure 6. Denote this frontier by F , and let Σ be $B \cap \partial H$, a sphere with four holes.

A *slope disk* for $\{\lambda, \rho\}$ is an essential disk in H , possibly separating, which is contained in $B - F$ and is not isotopic to any component of F . Any loop in Σ that is not homotopic into $\partial\Sigma$ is the boundary of a unique slope disk. (Throughout our work, “unique” means unique up to isotopy in an appropriate sense.) If two slope disks are isotopic in H , then they are isotopic in B . The boundary of a slope disk always separates Σ into two pairs of pants.

An arc in Σ whose endpoints lie in two different boundary circles of Σ is called a *cabling arc*. Figure 6 shows a pair of cabling arcs disjoint from a slope disk. A slope disk is disjoint from a unique pair of cabling arcs, and each cabling arc determines a unique slope disk.

Each choice of nonseparating slope disk for a pair $\mu = \{\lambda, \rho\}$ determines a correspondence between $\mathbb{Q} \cup \{\infty\}$ and the set of isotopy classes of slope disks of μ , as follows. Fixing a nonseparating slope disk τ for μ , write $(\mu; \tau)$ for the ordered pair consisting of μ and τ .

Definition 4.1. A *perpendicular disk* for $(\mu; \tau)$ is a disk τ^\perp , with the following properties:

- (i) τ^\perp is a slope disk for μ .
- (ii) τ and τ^\perp intersect transversely in one arc.
- (iii) τ^\perp separates H .

There are infinitely many choices for τ^\perp , but since $H \subset S^3$ there is a natural way to choose a particular one, which we call τ^0 . It is illustrated in Figure 7. To construct it, start with any perpendicular disk and change it by Dehn twists of H about τ until the core circles of the complementary solid tori have linking number 0 in S^3 .

For calculations, it is convenient to draw the picture as in Figure 7, and orient the boundaries of τ and τ^0 so that the orientation of τ^0 (the “ x -axis”), followed by the orientation of τ (the “ y -axis”), followed by the outward normal of H , is a right-hand orientation of S^3 . At the other intersection point, these give the left-hand orientation. The coordinates will be unaffected by changing which of the disks in $\{\lambda, \rho\}$ is called λ and which is ρ .

Let $\tilde{\Sigma}$ be the covering space of Σ such that:

- (i) $\tilde{\Sigma}$ is the plane with an open disk of radius $1/8$ removed at each point with coordinates in $\mathbb{Z} \times \mathbb{Z} + (\frac{1}{2}, \frac{1}{2})$.

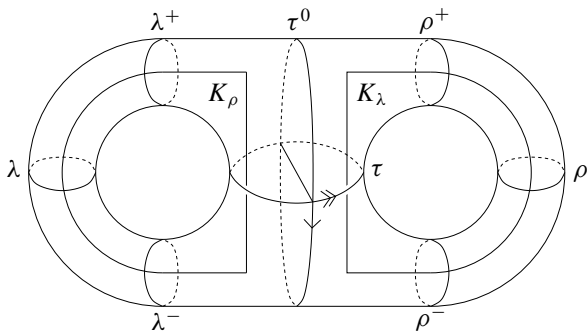


Figure 7. The slope-zero perpendicular disk τ^0 . It is chosen so that K_λ and K_ρ have linking number 0.

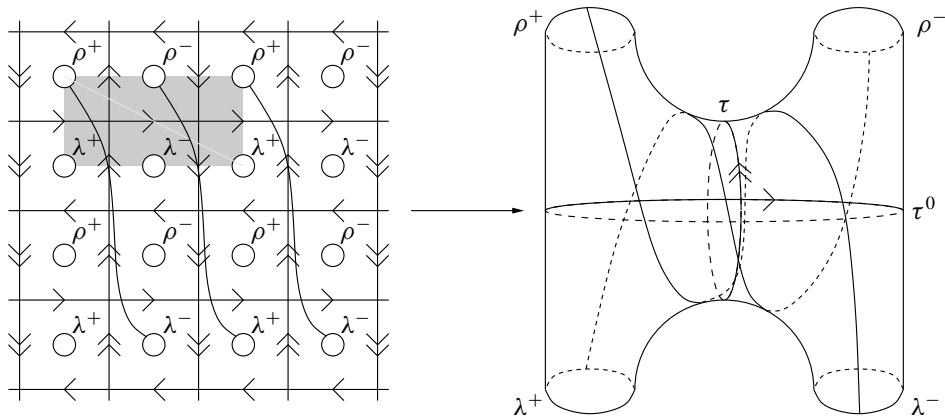


Figure 8. The covering space $\tilde{\Sigma} \rightarrow \Sigma$, and some lifts of the pair of $[1, -3]$ -cabling arcs from [Figure 6](#). The shaded region is a fundamental domain.

- (ii) The components of the preimage of τ are the vertical lines with integer x -coordinate.
- (iii) The components of the preimage of τ^0 are the horizontal lines with integer y -coordinate.

[Figure 8](#) shows a picture of $\tilde{\Sigma}$ and a fundamental domain for the action of its group of covering transformations, which is the orientation-preserving subgroup of the group generated by reflections in the half-integer lattice lines (that pass through the centers of the missing disks). Each circle of $\partial\tilde{\Sigma}$ double covers a circle of $\partial\Sigma$.

Each lift of a cabling arc α of Σ to $\tilde{\Sigma}$ runs from a boundary circle of $\tilde{\Sigma}$ to one of its translates by a vector (p, q) of signed integers, defined up to multiplication by the scalar -1 . In this way α receives a *slope pair* $[p, q] = \{(p, q), (-p, -q)\}$, and is called a $[p, q]$ -cabling arc. The corresponding slope disk is assigned the slope pair $[p, q]$ as well, and can be called a $[p, q]$ -slope disk. The cabling arcs in

Figure 8 are $[1, -3]$ -cabling arcs. A corresponding $[1, -3]$ -slope disk is the one shown in Figure 6.

An important observation is that a $[p, q]$ -slope disk is nonseparating in H if and only if q is odd. Both happen exactly when a corresponding cabling arc has one endpoint in λ^+ or λ^- and the other in ρ^+ or ρ^- .

Definition 4.2. Let λ , ρ , and τ be as above, and let $\mu = \{\lambda, \rho\}$. The $(\mu; \tau)$ -slope of a $[p, q]$ -slope disk or cabling arc is $q/p \in \mathbb{Q} \cup \{\infty\}$.

The $(\mu; \tau)$ -slope of τ^0 is 0, the $(\mu; \tau)$ -slope of τ is ∞ , and the $(\mu; \tau)$ -slope of a slope disk that looks like the one in Figure 6 is -3 . The $(\mu; \tau)$ -slope can also be called the $\{\tau, \tau^0\}$ -slope, when the choice of μ is clear.

Slope disks for a primitive pair are called *simple* disks, and are handled in a special way. Rather than using a particular choice of τ from the context, one chooses τ to be some third primitive disk. Altering this choice can change $[p, q]$ to any $[p+nq, q]$, but the quotient p/q is well-defined as an element of $\mathbb{Q}/\mathbb{Z} \cup \{\infty\}$. This element $[p/q]$ is called the *simple slope* of the slope disk. For example, if μ is a primitive pair, the simple slope of the disk from Figure 6 is $[2/3]$. The simple slope of a slope disk is $[0]$ exactly when the slope disk is itself primitive. Simple disks have the same simple slope exactly when they are equivalent by an element of the Goeritz group.

5. The cabling construction

In a sentence, the cabling construction (sometimes just called a *cabling*) is to “Think of the union of K and the tunnel arc as a θ -curve, and rationally tangle the ends of the tunnel arc and one of the arcs of K in a neighborhood of the other arc of K .” We sometimes call this “swap and tangle,” since one of the arcs in the knot is exchanged for the tunnel arc, then the ends of other arc of the knot and the tunnel arc are connected by a rational tangle.

Figure 9 illustrates two cablings, one starting with the trivial knot and obtaining the trefoil, then another starting with the tunnel of the trefoil.

More precisely, begin with a triple $\{\lambda, \rho, \tau\}$, regarded as a pair $\mu = \{\lambda, \rho\}$ with a slope disk τ which represents a tunnel. Choose one of the disks in $\{\lambda, \rho\}$, say λ , and a nonseparating slope disk τ' of the pair $\{\lambda, \tau\}$, *other than* ρ . This is a cabling operation producing the tunnel τ' from τ . In terms of the “swap and tangle” description of a cabling, λ is dual to the arc of K_τ that is retained, and the slope disk τ' determines a pair of cabling arcs that form the rational tangle that replaces the arc of K_τ dual to ρ .

Provided that $\{\lambda, \rho, \tau\}$ was not a primitive triple, we define the *slope* of this cabling operation to be the $(\{\lambda, \tau\}; \rho)$ -slope of τ' . When $\{\lambda, \rho, \tau\}$ is primitive, the cabling construction starts with the tunnel of the trivial knot and produces an upper

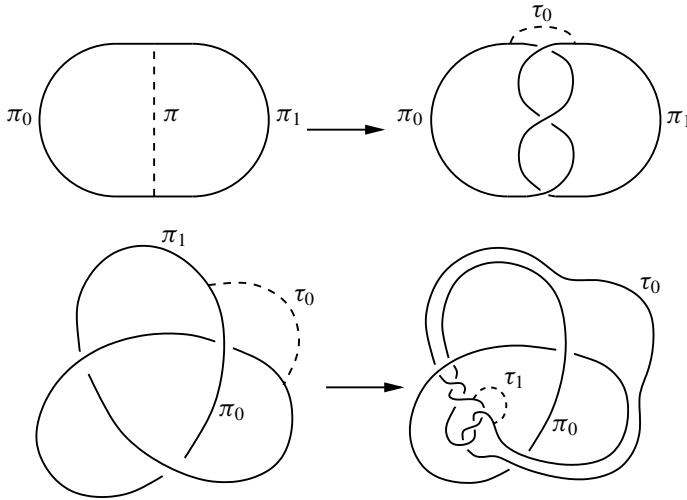


Figure 9. Examples of the cabling construction.

or lower tunnel of a 2-bridge knot, unless τ' is primitive, in which case it is again the tunnel of the trivial knot and the cabling is called *trivial*. The slope of a cabling starting with a primitive triple is defined to be the simple slope of τ' . The cabling is trivial when the simple slope is $[0]$.

Since tunnel disks for knot tunnels are nonseparating, the slope invariant of a cabling construction producing a knot tunnel is of the form q/p with q odd (or $[p/q]$ with q odd, for a simple slope). In this paper, all cablings will use nonseparating disks and produce knots. In general, a cabling construction can also use a separating disk as τ' , which will produce a tunnel of a tunnel number 1 link, and no further cabling is then possible. The slope invariant of such a cabling is defined in the same way, and has q even.

A nontrivial tunnel τ_0 produced from the tunnel of the trivial knot by a single cabling construction is called a *simple* tunnel. These are the well-known “upper and lower” tunnels of 2-bridge knots. Not surprisingly, the simple slope m_0 is a version of the standard rational parameter that classifies the 2-bridge knot K_{τ_0} .

A tunnel is called *semisimple* if it is disjoint from a primitive disk, but not from any primitive pair. The simple and semisimple tunnels are exactly the $(1, 1)$ -tunnels, that is, the upper and lower tunnels of knots in 1-bridge position with respect to a standard torus of S^3 . A tunnel is called *regular* if it is neither primitive, simple, or semisimple.

6. The tunnel invariants and the principal vertex

Theorem 13.2 of [Cho and McCullough 2009a] shows that every tunnel of every tunnel number 1 knot can be obtained by a uniquely determined sequence of cabling

constructions. The associated cabling slopes form a sequence

$$m_0, m_1, \dots, m_n = [p_0/q_0], q_1/p_1, \dots, q_n/p_n$$

where $m_0 \in \mathbb{Q}/\mathbb{Z}$ and each q_i is odd, called the sequence of *slope invariants* of the tunnel, or just its *slope sequence*.

The unique sequence of cabling constructions producing a tunnel τ begins with a primitive triple $\{\lambda_{-1}, \rho_{-1}, \tau_{-1}\}$, where τ_{-1} is regarded as the tunnel of the trivial knot. The cabling constructions produce triples $\{\lambda_i, \rho_i, \tau_i\}$ for $0 \leq i \leq n$, each $\{\lambda_i, \rho_i, \tau_i\}$ is either $\{\lambda_{i-1}, \tau_{i-1}, \tau_i\}$ or $\{\tau_{i-1}, \rho_{i-1}, \tau_i\}$. The triple $\{\lambda_n, \rho_n, \tau_n\}$ is called the *principal vertex* of τ . (It is called a vertex because it corresponds to a vertex in the “tree of knot tunnels” of [Cho and McCullough 2009a]). The uniqueness of the sequence of cabling constructions producing τ is really just the fact that in this tree there is a unique arc between any two vertices — in this case the unique vertex corresponding to the primitive triple and the nearest vertex containing τ — and each cabling construction corresponds to a step along this arc.

As we noted in Section 3, the principal vertex is dual to a specific isotopy class of θ -curves in S^3 . The arc of this θ -curve that is dual to the tunnel disk furnishes a canonical tunnel arc representing the tunnel (and the other two arcs form the knot). Indeed, each of the triples $\{\lambda_i, \rho_i, \tau_i\}$ determines the canonical tunnel arc representative of the tunnel τ_i . Geometrically, each cabling construction along the way produces the canonical tunnel arc of the resulting tunnel.

There is a second set of invariants associated to a tunnel. Each m_i is the slope of a cabling that begins with a triple of disks $\{\lambda_{i-1}, \rho_{i-1}, \tau_{i-1}\}$ and finishes with $\{\lambda_i, \rho_i, \tau_i\}$. For $i \geq 2$, put $s_i = 1$ if $\{\lambda_i, \rho_i, \tau_i\} = \{\tau_{i-2}, \tau_{i-1}, \tau_i\}$, and $s_i = 0$ otherwise. In terms of the swap-and-tangle construction, the invariant s_i is 1 exactly when the rational tangle replaces the arc of the knot that was retained by the previous cabling (for $i = 1$, the choice does not matter, as there is an element of the Goeritz group that preserves τ_0 and interchanges λ_0 and ρ_0).

A tunnel is simple or semisimple if and only if all $s_i = 0$. The reason is that both conditions characterize cabling sequences in which one of the original primitive disks is retained in every cabling; this corresponds to the fact that there exists a tunnel arc for the tunnel (the canonical tunnel arc, in fact) whose union with one of the arcs of the knot is unknotted.

7. Standard tangles

As we have seen, the cabling construction involves the replacement of a portion of a knot by a rational tangle in the ball B . In our later slope calculations, the rational tangle is positioned in B according to the picture seen in Figure 10, which we call a standard tangle. Notice that a standard tangle is isotopic (keeping endpoints in

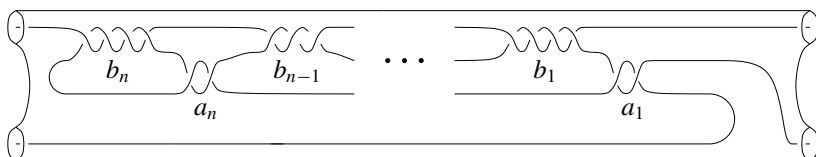


Figure 10. A standard tangle of type $(a_1, b_1, \dots, a_n, b_n)$. For a_i , each left-hand half-twist counts as $+1$, while for b_i , each right-hand half-twist does.

the frontier of B) to a unique pair of cabling arcs. So it makes sense to speak of the slope of a standard tangle. The next proposition gives a simple expression for this slope.

Proposition 7.1. *In the coordinates coming from the pair $\{\tau, \tau^0\}$ shown in the first drawing in Figure 11, the standard tangle of type $(a_1, b_1, \dots, a_n, b_n)$ has slope given by the continued fraction $[a_1, b_1, \dots, a_n, b_n]$.*

Proof. We write $U = \begin{bmatrix} 1 & 1 \\ 0 & 1 \end{bmatrix}$ and $L = \begin{bmatrix} 1 & 0 \\ 1 & 1 \end{bmatrix}$, and refer to Figure 11. The pair of arcs in the first picture of B has slope ∞ , and performing b_n left-hand half-twists of the right half of B produces the pair in the second picture, which has slope coordinates $[b_n, 1]$. Regarding a pair of slope coordinates $[p, q]$ as a column vector $\begin{bmatrix} q \\ p \end{bmatrix}$, this is expressed algebraically by the calculation

$$L^{b_n} \begin{bmatrix} 1 \\ 0 \end{bmatrix} = \begin{bmatrix} 1 & 0 \\ b_n & 1 \end{bmatrix} \begin{bmatrix} 1 \\ 0 \end{bmatrix} = \begin{bmatrix} 1 \\ b_n \end{bmatrix},$$

in which the resulting column vector gives the slope coordinates of the resulting cable. Next, we perform a_n right-hand half-twists of the bottom half of B . As seen in the third, fourth, and fifth pictures of Figure 11, this moves the arcs to the standard tangle of type (a_n, b_n) . The effect of a right-hand half-twist on slope coordinates is to send $[p, q]$ to $[p, q + p]$, which is the effect of multiplication by

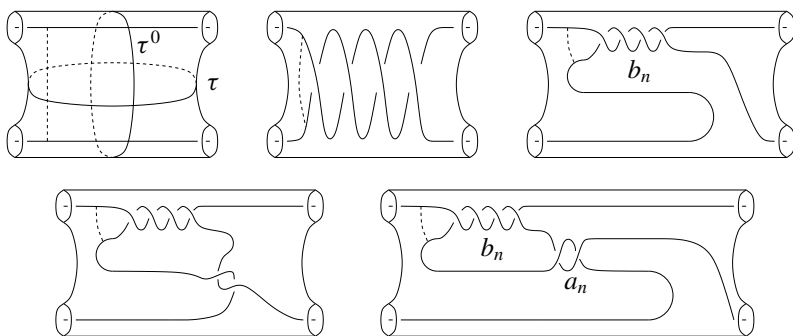


Figure 11. Calculating the slope of a standard tangle.

U . So the resulting slope coordinates from a_n twists are

$$U^{a_n} L^{b_n} \begin{bmatrix} 1 \\ 0 \end{bmatrix} = \begin{bmatrix} 1 & a_n \\ 0 & 1 \end{bmatrix} \begin{bmatrix} 1 \\ b_n \end{bmatrix} = \begin{bmatrix} 1 + a_n b_n \\ b_n \end{bmatrix},$$

and the slope is $a_n + 1/b_n = [a_n, b_n]$. An inductive calculation shows that

$$U^{a_1} L^{b_1} \dots U^{a_n} L^{b_n} \begin{bmatrix} 1 \\ 0 \end{bmatrix} = \begin{bmatrix} q \\ p \end{bmatrix}$$

where $q/p = [a_1, b_1, \dots, a_n, b_n]$ [Cho and McCullough 2009a, Lemma 14.3], verifying the proposition. \square

8. Unwinding rational tangles

In this section, we introduce two isotopy maneuvers similar to the one in Section 2. They reposition a knot that is produced by a cabling construction on a knot and tunnel in the standard position detailed in Section 2. This leads to our first main result, Theorem 8.1, which tells how performing a cabling construction on an upper tunnel in standard position changes a braid description of the $(1, 1)$ -position.

Figure 12(a) shows a knot and tunnel produced by a cabling construction, starting from a tunnel in the standard position seen in Figure 5(c). Notice that the original tunnel arc seen in Figure 5(c) now appears as an arc of the new knot — this is the “swap” part of the cabling construction. The arc labeled α_W in Figure 5(c), that was an arc of the original knot, is replaced by a standard tangle in the position shown in Figure 12(a). The new tunnel arc is the dotted arc at the lower left of the two-bridge configuration. Provided that the original tunnel arc was the canonical tunnel arc of the original knot, the new tunnel arc is the canonical tunnel arc of the

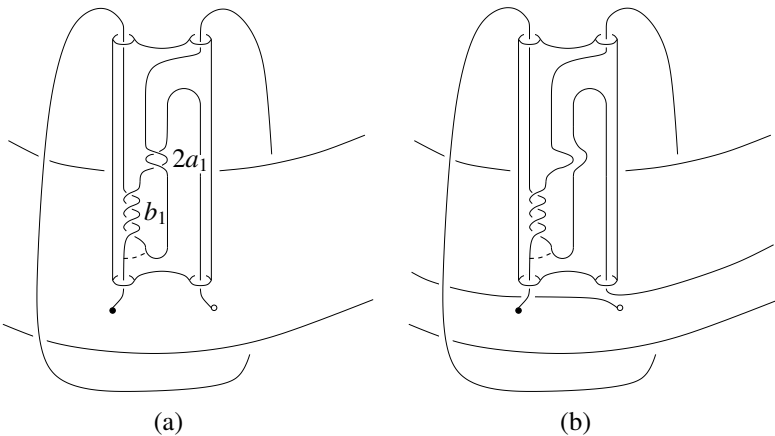


Figure 12. Unwinding full twists of the middle two strands.

new knot. This is because the cablings in the unique sequence producing a tunnel produce the canonical tunnel arcs for each tunnel (see [Section 6](#)).

The knot resulting from this cabling construction depends on the element $\omega \in \mathcal{B}$, not just on its double coset $\langle \delta_\ell, \sigma \rangle \omega \langle \delta_m, \sigma \rangle$.

Since the slope of any cabling producing a knot (rather than a two-component link) is of the form q/p with q odd, Lemma 14.2 of [[Cho and McCullough 2009a](#)] shows that q/p has a continued fraction expansion of the form

$$[2a_1, b_1, 2a_2, b_1, \dots, 2a_n, b_n].$$

So we can and will assume that the standard tangle in [Figure 12](#) has type of the form $(2a_1, b_1, 2a_2, \dots, 2a_n, b_n)$, and consequently the middle two strands in the tangle have only full twists.

The first maneuver unwinds one left-hand full twist of the middle two strands at the top of the braid, adding a letter δ_ℓ^{-1} at the beginning of the braid description of the previous knot. During the isotopy, the knot cuts once across a core circle of W . The resulting knot is shown in [Figure 12\(b\)](#). If the twist is right-hand, the isotopy is similar but a letter δ_ℓ is added.

The second maneuver is possible when there are no twists of the middle two strands at the top of the braid, as in [Figures 12\(b\)](#) and [13\(a\)](#). It is similar to the first maneuver, but unwinds half-twists of the left two strands at the expense of adding initial powers of σ to ω . During the isotopy, the knot need not pass through a core circle of W ; it can be fixed outside a small neighborhood of the ball B that contains the standard tangle. As seen in [Figure 13\(b\)](#), unwinding a single half-twist adds an initial letter σ or σ^{-1} to the braid description, according as the half-twist is right-handed or left-handed.

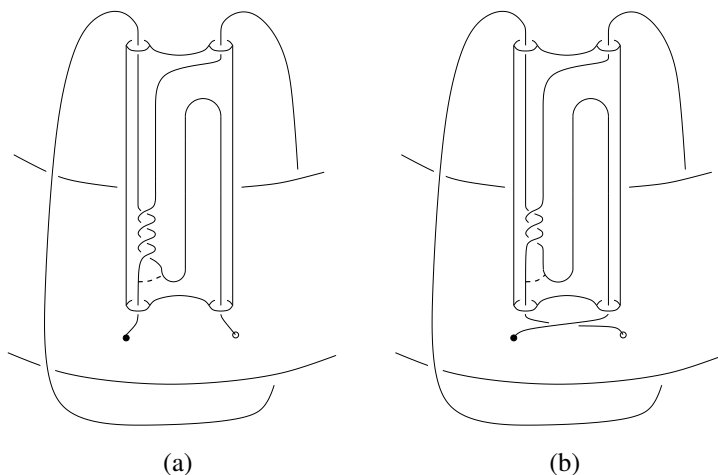


Figure 13. Unwinding half-twists of the left two strands.

If there are additional twists of the middle or left strands lying below those shown in Figure 12, they can be unwound by repeating the previous two maneuvers. Thus the sequence of full twists of the middle two strands and half-twists of the left two strands unwinds to add $\sigma^{b_n} \delta_\ell^{-a_n} \dots \sigma^{b_1} \delta_\ell^{-a_1}$ at the start of the braid description. The knot and tunnel are then in the position in Figure 5(a), and the maneuver of Section 2 puts the knot and tunnel into the standard position of Figure 5(c), adding $\delta_m \sigma$ to the front of the braid description. This establishes our first main result:

Theorem 8.1 (Unwinding theorem). *Suppose that a (1, 1)-knot K and its upper (1, 1)-tunnel are in standard position with braid description $w \in \mathfrak{B}$. Perform a cabling construction that introduces a standard tangle of type $(2a_1, b_1, \dots, 2a_n, b_n)$, positioned as shown in Figure 12. Then using (1, 1)-isotopy, the new knot and tunnel can be put into standard position with braid description*

$$\delta_m \sigma \cdot \sigma^{b_n} \delta_\ell^{-a_n} \sigma^{b_{n-1}} \dots \sigma^{b_1} \delta_\ell^{-a_1} \cdot w.$$

9. The slope theorem

To calculate the slope invariant of a cabling as in Figure 12, we must find the slope-zero perpendicular disk ρ^0 of ρ , where ρ is the slope disk in Figure 14(a). Then we determine the $\{\rho, \rho^0\}$ -slope of the standard tangle of type $(2a_1, b_1, \dots, 2a_n, b_n)$. In this section, we will carry these out, leading to our second main result, Theorem 9.3. It gives a simple expression for the slope of a cabling construction of the type considered in Theorem 8.1. The expression involves an integer that counts the number of turns the knot makes around the solid torus $T \times I \cup V$. Definition 9.1 and Proposition 9.2 will show how to compute this integer from a braid description of the (1, 1)-position.

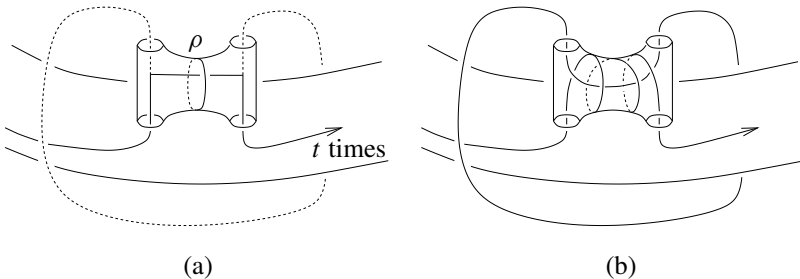


Figure 14. Finding the slope-zero perpendicular disk ρ^0 . The first drawing (a) shows ρ and indicates the direction of algebraically positive winding of the knot around V . The second (b) shows the 0-linking pair for ρ^0 , for the case $t = 3$. The corresponding disk ρ^0 appears in Figure 15(b).

Assuming that the upper tunnel of K is in standard position as in Figure 5(c), we always choose the orientation on K to be directed over the top arch α_W from the black point to the white point. The *algebraic winding number* for this position of K is defined to be the net number of turns that K makes in the direction of positive orientation on the longitude ℓ of $T \times I \cup V$ (the direction indicated in Figure 14(a)), that is, the algebraic intersection of K with a meridian disk of $T \times I \cup V$ bounded by the loop m .

Definition 9.1. For $\omega \in \mathcal{B}$, define $t(\omega) \in \mathbb{Z}$ as follows. For each appearance of δ_ℓ^ϵ ($\epsilon = \pm 1$) in ω , write $\omega = \omega_1 \delta_\ell^\epsilon \omega_2$, and let k be the total exponent of σ in ω_1 . Assign the value $(-1)^{k+1} \epsilon$ to this appearance of δ_ℓ^ϵ , and sum these over all appearances to give $t(\omega)$.

Proposition 9.2. *If $K = K(\omega)$, then $t(\omega)$ equals the algebraic winding number of K .*

Proof. For our designated orientation on K and choice of direction of positive winding, an initial letter δ_ℓ in ω as in the example of Figure 3(a) would contribute -1 to the algebraic winding number of K . If it were δ_ℓ^{-1} it would contribute $+1$. When δ_ℓ^ϵ is not the initial letter, each of the appearances of σ preceding an appearance of δ_ℓ^ϵ in ω reverses the direction in which the orientation of K is directed around the turn corresponding to this δ_ℓ^ϵ term. So if there are k such appearances of σ , this appearance of δ_ℓ^ϵ contributes $(-1)^k (-\epsilon) = (-1)^{k+1} \epsilon$ to the algebraic winding number. Apart from this effect of σ on the signs of these terms, the appearances of δ_m and σ in ω make no contribution to the algebraic winding number. \square

We can now state our second main result.

Theorem 9.3 (Slope theorem). *Let $K = K(\omega)$ be a knot in braid position with upper tunnel in standard position as shown in Figure 5(c). Suppose that a cabling construction as in Figure 12 is performed using a standard tangle of type $(2a_1, b_1, \dots, 2a_n, b_n)$. Then the slope of the cabling is given by the continued fraction $[2t(\omega) + 2a_1, b_1, 2a_2, \dots, b_n]$.*

Proof. Figure 14(b) shows the link formed by the core circles of the solid tori into which the slope disk in Figure 15(b) will cut a handlebody neighborhood of the union of the knot and the tunnel. The lower component is $(1, 1)$ -isotopic to K , while the upper component is a core circle of the solid torus W . Let t be the number of full left-handed twists of the right half of B needed to change the disk ρ^\perp in Figure 15(a) to the disk in Figure 15(b). Recalling that the algebraic winding number of K is its algebraic intersection number with a meridian disk of $T \times I \cup V$, we see that the linking number of the lower component with the upper component is t less than the algebraic winding number of K . If we choose t to equal this algebraic winding number, then the linking number will be 0, and therefore

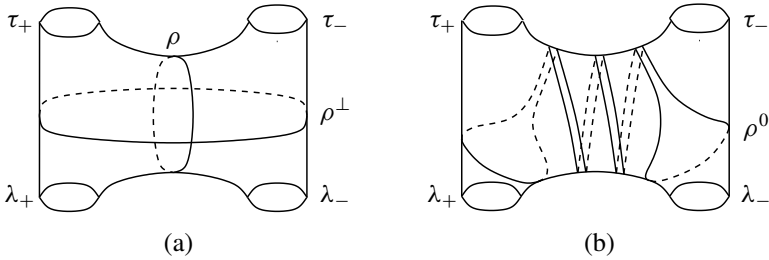


Figure 15. A perpendicular disk ρ^\perp and the slope-zero perpendicular disk ρ^0 for the case $t = 3$.

the disk in [Figure 15\(b\)](#) will be the canonical zero-slope disk ρ^0 . According to [Proposition 9.2](#), the algebraic winding number of K is $t(\omega)$, so the condition is that $t = t(\omega)$.

Now consider a standard tangle K_0 of type $(2a_1, b_1, \dots, 2a_n, b_n)$, as shown in [Figure 10](#). Regard it as contained in the portion of the handlebody shown in [Figure 15](#), as in [Figure 12](#). [Proposition 7.1](#) gives the slope of K_0 with respect to the pair $\{\rho, \rho^\perp\}$ in [Figure 15\(a\)](#) to be $[2a_1, b_1, \dots, 2a_n, b_n]$. We denote this slope by $m(K_0, \{\rho, \rho^\perp\})$, and by $m(K_0, \{\rho, \rho^0\})$ the slope with respect to $\{\rho, \rho^0\}$.

Let u denote a full left-hand twist of the right-hand side of the ball in [Figure 15](#). We have already seen that $u^t(\rho^\perp) = \rho^0$, and we note also that $u^t(\rho) = \rho$. In the view of [Figure 10](#), u is a full left-hand twist of the bottom half of B , so u^{-t} moves K_0 to the standard tangle of type $(2t + 2a_1, b_1, 2a_2, b_2, \dots, 2a_n, b_n)$. We can now compute the slope of the cabling as

$$\begin{aligned} m(K_0, \{\rho, \rho^0\}) &= m(K_0, \{\rho, u^t(\rho^\perp)\}) = m(K_0, \{u^t(\rho), u^t(\rho^\perp)\}) \\ &= m(u^{-t}(K_0), \{\rho, \rho^\perp\}) = [2t + 2a_1, b_1, \dots, 2a_n, b_n] \end{aligned}$$

where [Proposition 7.1](#) gives the final equality. \square

Example 9.4. [Figure 16](#) shows the knot of [Figure 9](#) of [[Cho and McCullough 2009a](#)] moved into $(1, 1)$ -position. The upper right-hand drawing is the original knot and its upper and lower tunnels τ_1 and τ_2 . In the $(1, 1)$ -position in [Figure 9](#) of [[Cho and McCullough 2009a](#)], τ_2 is the upper tunnel. From the bottom-right drawing, we read off a braid description of τ_2 as $\omega = \delta_m^{-1} \sigma^{-1} \delta_\ell \delta_m^{-1} \sigma^3 \delta_\ell^{-1} = \sigma \delta_m \delta_\ell \delta_m^{-1} \sigma^3 \delta_\ell^{-1} \sim \delta_m \delta_\ell \delta_m^{-1} \sigma^3 \delta_\ell^{-1}$.

To compute the slope invariants for the tunnel τ_2 , we use the relation $\delta_m^{-1} = \sigma \delta_m \sigma$ to put ω into the form

$$\delta_m \sigma \cdot \omega_1(\delta_\ell, \sigma) \cdot \delta_m \sigma \cdot \omega_0(\delta_\ell, \sigma) = \delta_m \sigma \cdot \sigma^{-1} \delta_\ell \sigma \cdot \delta_m \sigma \cdot \sigma^3 \delta_\ell^{-1}.$$

We now use [Theorems 8.1](#) and [9.3](#) to read off the slopes. The first cabling starts from the trivial knot K , which has algebraic winding number $t(1) = 0$. Since the

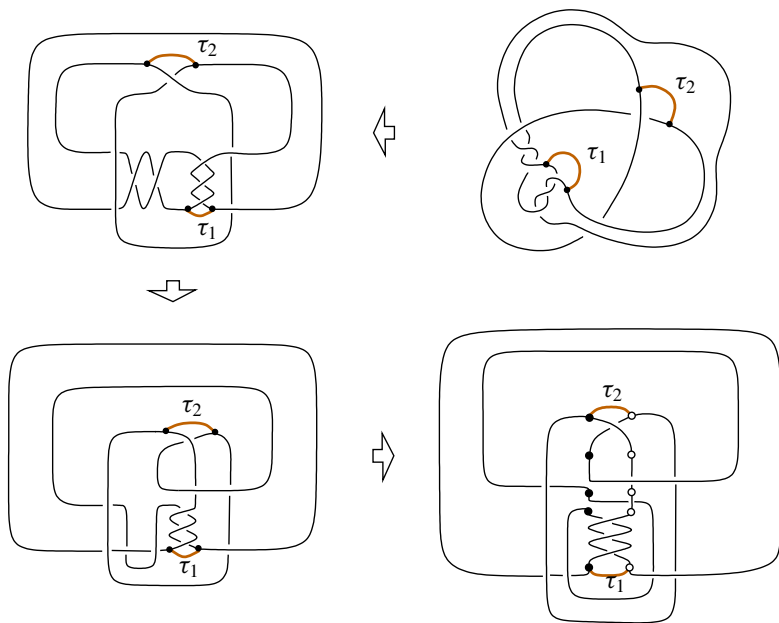


Figure 16. Putting a knot into $(1, 1)$ -position.

cabling corresponds to the portion $\delta_m \sigma \cdot \omega_0(\delta_\ell, \sigma) = \delta_m \sigma \cdot \sigma^3 \delta_\ell^{-1}$, [Theorem 8.1](#) shows that the standard tangle used in the cabling is of type $(2a_1, b_1) = (2, 3)$. By [Theorem 9.3](#), the ordinary slope of the first cabling is given by the continued fraction $[0 + 2, 3] = 7/3$, so the simple slope is $[3/7]$ in \mathbb{Q}/\mathbb{Z} . The second cabling begins with this knot, so has algebraic winding number $t(\delta_m \sigma \cdot \sigma^3 \delta_\ell^{-1}) = (-1)^{4+1} \cdot (-1) = 1$. From [Theorem 8.1](#), we have $a_1 = 0, b_1 = 1, a_2 = -1$, and $b_2 = -1$, so by [Theorem 9.3](#) the second cabling slope is given by the continued fraction $[2 + 0, 1, -2, -1] = 7/2$. Therefore the slope sequence of τ_2 is $[3/7], 7/2$.

The tunnel τ_1 is the upper tunnel of the $(1, 1)$ -position described by the reverse braid of ω ,

$$\delta_m^{-1} \sigma^3 \delta_\ell^{-1} \delta_m \delta_\ell \sim \delta_m \sigma \cdot \sigma^3 \delta_\ell^{-1} \cdot \delta_m \sigma \cdot \sigma^{-1} \delta_\ell,$$

giving the first slope of τ_1 to be $[0 + (-2), -1] = -3$ and consequently its simple slope to be $[-1/3] = [2/3] \in \mathbb{Q}/\mathbb{Z}$. For the second slope, we have $t(\delta_m \delta_\ell) = (-1)^{0+1} \cdot 1 = -1$, $a_1 = 1$, and $b_1 = 3$, giving the slope $[2 \cdot (-1) + 2, 3] = 1/3$. Therefore the cabling slope sequence of the lower tunnel is $[2/3], 1/3$.

10. Tunnels of 2-bridge knots

In this section we will give braid descriptions of the tunnels of 2-bridge knots, and use them to calculate the slope invariants. We obtain, of course, the same values as

in the calculation of [Cho and McCullough 2009a, Section 15]. In Theorem 10.5 we give a characterization of which sequences of rational numbers (with initial term in \mathbb{Q}/\mathbb{Z}) occur as slope sequences of tunnels of 2-bridge knots.

A convenient reference for the tunnels of 2-bridge knots is [Morimoto and Sakuma 1991, Section (1.6)]. In [ibid., Section (1.1)], the authors give a definition of *dual* tunnels, and the discussion in [ibid., Section (1.2)] shows that two tunnels of a knot in S^3 are dual exactly when they are the upper and lower tunnels for the same $(1, 1)$ -position of the knot. As we saw in Section 1, the dual of a tunnel given by a braid description ω has a braid description by the reverse braid of ω .

Figure 17 shows a 2-bridge knot, where the regions labeled $2a_i$ indicate $2a_i$ left-hand half-twists and those labeled b_i indicate b_i right-hand half-twists. The upper, lower, upper semisimple, and lower semisimple tunnels are shown; from [ibid., Section (1.6)], the upper semisimple and lower simple tunnels are dual, as are the lower semisimple and upper simple tunnels.

This position is assigned to the rational number a/b given by the continued fraction $[2a_1, b_1, 2a_2, \dots, 2a_n, b_n]$. Changing the position by $(1, 1)$ -isotopy if need be, we may assume that $2a_1$ and b_n are nonzero (indeed we may assume that no a_i or b_i is zero, although for some calculations it is convenient to allow zero values), and we always choose a positive, so have $0 < |b| < a$. Also, a is odd (the values when a is even correspond to 2-bridge links).

Notice that there is an isotopy moving the knot in Figure 17 to the position given by the continued fraction $[-b_n, -2a_n, -b_{n-1}, \dots, -b_1, -2a_1]$. The first step is to move the top horizontal strand down to the bottom. The twists b_i then appear in the middle and the $2a_i$ at the top. Then the entire knot is rotated until it looks as in Figure 17 except with the twists b_i in the middle and the $2a_i$ at the bottom; the minus signs are due to the convention about which directions of twists are considered to be positive for the middle versus the bottom two strands. The upper tunnel for the second position is the lower tunnel for the original position. Similarly, the upper semisimple tunnel for the first position is the lower semisimple tunnel for the second.

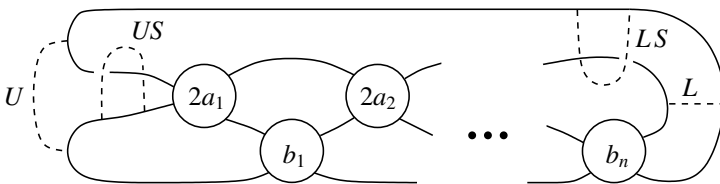


Figure 17. A 2-bridge knot with classifying invariant given by the continued fraction $1/[2a_1, b_1, 2a_2, \dots, 2a_n, b_n]$. The upper and lower tunnels U and L and the upper and lower semisimple tunnels US and LS are shown.

If $[2a_1, b_1, \dots, 2a_n, b_n] = a/b$, then $[-b_n, -2a_n, -b_{n-1}, \dots, -b_1, -2a_1]$ is a/b' where $0 < |b| < a$, $0 < |b'| < a$, and $bb' \equiv 1 \pmod{a}$. This and many other basic facts about continued fraction expansions can be verified using Lemma 14.3 of [Cho and McCullough 2009a]. For suppose we use Lemma 14.2 of that reference (which is itself a consequence of Lemma 14.3) to write $[2a_1, b_1, \dots, 2a_n, b_n] = a/b$. By Lemma 14.3, we have $U^{2a_1} L^{b_1} \dots U^{2a_n} L^{b_n} = \begin{bmatrix} a & r \\ b & s \end{bmatrix}$, where

$$[-b_n, -2a_n, -b_{n-1}, \dots, -b_1, -2a_1] = -[b_n, 2a_n, b_{n-1}, \dots, b_1, 2a_1] = a/(-r).$$

Since $as - rb = 1$, we have $(-r)b = 1 \pmod{a}$.

The 2-bridge knot is actually classified up to isotopy by the pair of (possibly equal) values b/a and b'/a in \mathbb{Q}/\mathbb{Z} . Replacing a/b by $a/(b \pm a)$, if necessary, and applying Lemma 14.2 of [Cho and McCullough 2009a], we may assume that all terms in the continued fraction expansion of a/b are even. The corresponding 2-bridge position, having only full twists of the left two strands and the middle two strands, is called the *Conway position* of the 2-bridge knot.

Proposition 10.1. *The lower simple tunnel has slope invariant*

$$m_0 = [1/[2a_1, b_1, \dots, 2a_n, b_n]],$$

and the upper simple tunnel has slope invariant

$$m_0 = [1/[-b_n, -2a_n, -b_{n-1}, \dots, -b_1, -2a_1]].$$

Proof. Figure 18, a case of Figure 12(a), shows a 2-bridge knot K obtained from the trivial knot K_0 by a single cabling. The tunnel arc is the lower simple tunnel of K . Since the algebraic winding number $t(K_0)$ is 0, Theorem 9.3 gives the slope of this cabling to be $[2a_1, b_1, \dots, 2a_n, b_n]$, so the simple slope of the lower tunnel is $[1/[2a_1, b_1, \dots, 2a_n, b_n]]$. Since the upper simple tunnel is the lower simple tunnel for the position of K corresponding to the continued fraction $[-b_n, -2a_n, -b_{n-1}, \dots, -b_1, -2a_1]$, the simple slope of the upper tunnel is as given in the proposition. (To apply Theorem 9.3, the position would have to be moved by isotopy to change the $-b_i$ to be even, but this would not change the value of the continued fraction.) \square

From Proposition 10.1, we have:

Corollary 10.2. *Let the rational invariant of the 2-bridge knot be given by the continued fraction $a/b = [2a_1, b_1, 2a_2, \dots, 2a_n, b_n]$, with $0 < b < a$. Let b' be the integer with $0 < b' < a$ and $bb' \equiv 1 \pmod{a}$. Then the simple slope of the upper tunnel of K is $[b'/a]$, and the simple slope of the lower tunnel is $[b/a]$.*

We turn now to the semisimple tunnels, whose slope invariants were calculated in [Cho and McCullough 2009a]. We will obtain a braid description such that the upper semisimple tunnel is the upper tunnel for the associated $(1, 1)$ -position, then

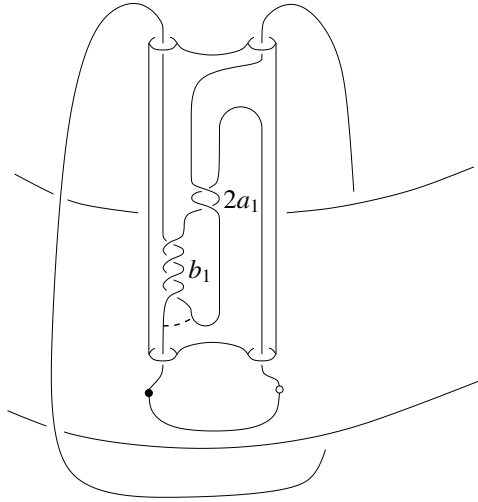


Figure 18. The slope calculation for the lower tunnel of a 2-bridge knot.

use it to recover the slope calculation of [Cho and McCullough 2009a]. We will also prove a new result, [Theorem 10.5](#), which characterizes the slope sequences of these tunnels.

Braid descriptions of these $(1, 1)$ -positions were given by A. Cattabriga and M. Mulazzani [2004] and more recently in the dissertation of A. Seo [2008]. Here is the braid description that we will use:

Lemma 10.3. *The braid word $\delta_m^{-a_1} \sigma^{b_1} \dots \delta_m^{-a_n} \sigma^{b_n} \delta_\ell^{-1}$ describes a $(1, 1)$ -position of the 2-bridge knot K given by $[2a_1, b_1, \dots, 2a_n, b_n]$. The upper tunnel of this $(1, 1)$ -position is the upper semisimple tunnel of K .*

A quick way to obtain this braid description is to use the fact that the upper semisimple tunnel is dual to the lower simple tunnel. As seen in [Figure 18](#), the lower simple tunnel is obtained from the upper tunnel of the trivial knot by a single cabling of type $(2a_1, b_1, \dots, 2a_n, b_n)$. By [Theorem 8.1](#), this $(1, 1)$ -position is described by the braid $\delta_m \sigma^{b_n+1} \delta_\ell^{-a_n} \dots \sigma^{b_1} \delta_\ell^{-a_1}$. Since the upper semisimple tunnel is dual to the lower simple tunnel, it is the upper tunnel of the $(1, 1)$ -position described by the reverse of this word, which is

$$\delta_m^{-a_1} \sigma^{b_1} \dots \delta_m^{-a_n} \sigma^{b_n+1} \delta_\ell \sim \delta_m^{-a_1} \sigma^{b_1} \dots \delta_m^{-a_n} \sigma^{b_n} \delta_\ell^{-1}.$$

A second, perhaps more satisfying way to obtain [Lemma 10.3](#) is to see the braid directly. [Figure 19](#) shows the setup. The second drawing shows the view from inside W , similar to the view of [Figure 3](#), and the first shows the view from $T \times I$ looking at W from the outside. Observe that a full twist of the middle two strands

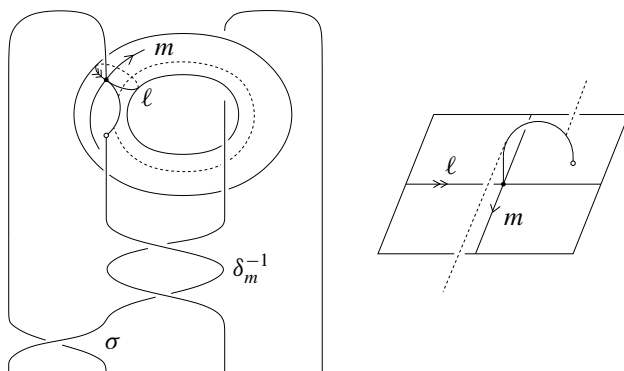


Figure 19. Calculation of the braid description for the upper semisimple tunnel of a 2-bridge knot, as seen from the outside and from the inside of the standard torus.

represents the braid that moves the white point around m in the positive direction, which is δ_m^{-1} , and the half-twist of the left two strands represents σ .

Figure 20 shows the tunnel of the trivial knot as the upper semisimple tunnel of the trivial 2-bridge knot. It is the upper tunnel for the $(1, 1)$ -position of the trivial knot described by the braid δ_ℓ^{-1} that moves the white point around ℓ in the positive direction, that is, $K(\delta_\ell^{-1})$.

Now, modify the trivial knot in **Figure 20** by inserting a standard tangle of type $(2a_1, b_1, \dots, 2a_n, b_n)$ into $T \times I$, in the position seen in **Figure 19**. The portion labeled δ_m^{-1} in **Figure 19** will be $2a_1$ left-hand half-twists, the portion labeled σ will be b_1 right-hand half-twists, below this will be $2a_2$ left-hand half-twists, and so on, ending with b_n half-twists and then the δ_ℓ^{-1} already present. This produces the knot seen in **Figure 17**, and the upper semisimple tunnel seen there, and the braid description of **Lemma 10.3**.

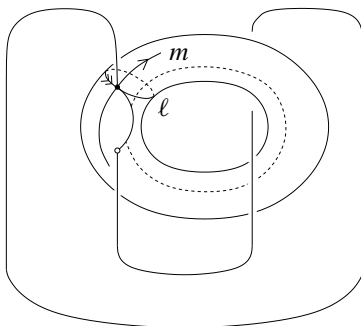


Figure 20. The initial position of the trivial tunnel as an upper semisimple tunnel has braid description δ_ℓ^{-1} .

We are now ready to calculate the slope invariants. By allowing the possibility that $b_i = 0$, we may assume that every a_i is ± 1 (since continued fractions have the property that $[\dots, n_1 + n_2, \dots] = [\dots, n_1, 0, n_2, \dots]$). We may further assume that if the last term $b_n = \pm 1$ then a_n and b_n have the same sign.

It is convenient to reindex the continued fraction as $[2a_d, b_d, 2a_{d-1}, \dots, 2a_0, b_0]$. We first consider four cases with $i \geq 1$:

Case I: $a_i = 1, a_{i-1} = 1$. In this case the braid appears as

$$\omega_1 \delta_m^{-1} \sigma^{b_i} \delta_m^{-1} \sigma^{b_{i-1}} \omega_2 = \omega_1 \sigma (\delta_m \sigma) \sigma^{b_i+1} \delta_m \sigma^{b_{i-1}+1} \omega_2$$

and the cabling corresponding to a_i has slope $[2t(\omega), b_i + 1]$, where

$$\omega = \delta_m \sigma^{b_{i-1}+1} \omega_2.$$

Case II: $a_i = -1, a_{i-1} = 1$. The braid is

$$\omega_1 \delta_m \sigma^{b_i} \delta_m^{-1} \sigma^{b_{i-1}} \omega_2 = \omega_1 (\delta_m \sigma) \sigma^{b_i} \delta_m \sigma^{b_{i-1}+1} \omega_2$$

and the cabling corresponding to a_i has slope $[2t(\omega), b_i]$, with ω as in Case I.

Case III: $a_i = 1, a_{i-1} = -1$. The braid is

$$\omega_1 \delta_m^{-1} \sigma^{b_i} \delta_m \sigma^{b_{i-1}} \omega_2 = \omega_1 \sigma (\delta_m \sigma) \sigma^{b_i} \delta_m \sigma^{b_{i-1}} \omega_2$$

and the cabling corresponding to a_i has slope $[2t(\omega), b_i]$, but this time

$$\omega = \delta_m \sigma^{b_{i-1}} \omega_2.$$

Case IV: $a_i = -1, a_{i-1} = -1$. The braid is

$$\omega_1 \delta_m \sigma^{b_i} \delta_m \sigma^{b_{i-1}} \omega_2 = \omega_1 (\delta_m \sigma) \sigma^{b_i-1} \delta_m \sigma^{b_{i-1}} \omega_2$$

and the cabling corresponding to a_i has slope $[2t(\omega), b_i - 1]$, with ω as in Case III.

For the initial cabling, we have

Case V: $a_0 = 1$. The braid is

$$\dots \sigma^{b_1} \delta_m^{-1} \sigma^{b_0} \delta_\ell^{-1} = \dots \sigma^{b_1+1} (\delta_m \sigma) \sigma^{b_0} \delta_\ell^{-1}$$

and the initial cabling has simple slope $[1/[2, b_0]] = [b_0/(2b_0 + 1)]$.

Case VI: $a_0 = -1$. The braid is

$$\dots \sigma^{b_1} \delta_m \sigma^{b_0} \delta_\ell^{-1} = \dots \sigma^{b_1} (\delta_m \sigma) \sigma^{b_0-1} \delta_\ell^{-1}$$

and the initial cabling has simple slope $[1/[2, b_0 - 1]] = [(b_0 - 1)/(2b_0 - 1)]$.

From [Cases V–VI](#), we have $m_0 = [b_0/(2b_0 + 1)]$ or $m_0 = [(b_0 - 1)/(2b_0 - 1)]$ according as a_0 is 1 or -1 .

To compute the remaining m_i , we assume that the knot is in Conway position so that all the b_i are even. We then have

$$t(\omega_2) = t(\delta_m^{-a_i-2} \sigma^{b_{i-2}} \dots \delta_m^{-a_0} \sigma^{b_0} \delta_\ell^{-1}) = (-1)^{b_{i-2} + \dots + b_0} = 1,$$

and from [Cases I–IV](#), using the fact that b_{i-1} is even, $t(\omega)$ equals -1 when $a_{i-1} = 1$ and 1 when $a_{i-1} = -1$. That is, $t(\omega) = -a_{i-1}$. Summarizing, we have

Proposition 10.4. *Let K be in the 2-bridge position corresponding to the continued fraction $[2a_d, 2b_d, \dots, 2a_0, 2b_0]$, with $b_0 \neq 0$ and each $a_i = \pm 1$. Then the slope invariants of the upper semisimple tunnel of K are as follows:*

- (i) $m_0 = \left[\frac{2b_0}{4b_0 + 1} \right]$ or $m_0 = \left[\frac{2b_0 - 1}{4b_0 - 1} \right]$ according as a_0 is 1 or -1 .
- (ii) For $1 \leq i \leq d$, $m_i = -2a_{i-1} + 1/k_i$, where
 - (a) $k_i = 2b_i + 1$ if $a_i = a_{i-1} = 1$,
 - (b) $k_i = 2b_i$ if a_i and a_{i-1} have opposite signs, and
 - (c) $k_i = 2b_i - 1$ if $a_i = a_{i-1} = -1$.

This agrees with the calculation obtained in Section 15 of [\[Cho and McCullough 2009a\]](#).

Using [Proposition 10.4](#), we can characterize the slope sequences of semisimple tunnels of 2-bridge knots.

Theorem 10.5. *Let m_0, m_1, \dots, m_d be a sequence with $m_0 \in \mathbb{Q}/\mathbb{Z}$ and $m_i \in \mathbb{Q}$ for $i > 0$. Then m_0, m_1, \dots, m_d is the slope sequence for a semisimple tunnel of a 2-bridge knot if and only if it satisfies the following:*

- (i) $m_0 = \left[\frac{n_0}{2n_0 + 1} \right]$ for some $n_0 \notin \{-1, 0\}$.
- (ii) For $i > 0$, $m_i = \pm 2 + \frac{1}{k_i}$ for some integer $k_i \neq 0$.
- (iii) m_1 is positive or negative according as n_0 is odd or even.
- (iv) For $1 \leq i \leq d$, m_i has the same sign as m_{i-1} if and only if k_{i-1} is odd.

Proof. First assume that this is a slope sequence for a semisimple tunnel. Part (i) follows from [Proposition 10.4\(i\)](#), with the excluded cases corresponding to the cases when $b_0 = 0$. Part (ii) is immediate from [Proposition 10.4\(ii\)](#). In [Proposition 10.4\(ii\)](#), m_1 has the opposite sign from a_0 , and [Proposition 10.4\(i\)](#) shows that a_0 is negative or positive according as n_0 is odd or even. This establishes part (iii). For part (iv), [Proposition 10.4\(ii\)](#) shows that the signs of m_i and m_{i-1} differ exactly when a_{i-1} and a_{i-2} have opposite signs. By [Proposition 10.4\(ii\)](#), this is exactly

the case when $k_{i-1} = 2b_{i-1}$, and when a_{i-1} and a_{i-2} have the same sign, $k_{i-1} = 2b_{i-1} \pm 1$ which is odd.

For the converse, given a sequence m_0, \dots, m_d as stated in the theorem, we will construct the continued fraction expansion $a/b = [2a_d, 2b_d, \dots, 2a_0, 2b_0]$ for the Conway position, with each $a_i = \pm 1$. Let a_0 be -1 or 1 according to whether n_0 is odd or even. For ascending i with $1 \leq i \leq d$, let a_i be a_{i-1} if k_i is odd, and $-a_{i-1}$ if it is even. For the b_i , put $2b_0 = n_0$ or $n_0 + 1$ according as n_0 is even or odd. **Cases I–IV** now determine the choices of the remaining $2b_i$ which produce the correct values for the m_i : When $a_i = -a_{i-1}$, k_i is even and **Cases II** and **III** give $2b_i = k_i$. When $a_i = a_{i-1}$, k_i is odd and **Cases I** and **IV** show that $2b_i = k_i - 1$ if $a_i = 1$ and $2b_i = k_i + 1$ if $a_i = -1$. \square

11. Semisimple tunnels of torus knots

To set notation, consider a (nontrivial) (p, q) -torus knot $K_{p,q}$, contained in our standard torus T . It represents p times a generator in $\pi_1(V \cup T \times I)$, and q times a generator in $\pi_1(W)$.

The tunnels of torus knots were classified by M. Boileau, M. Rost, and H. Zieschang [Boileau et al. 1988] and Y. Moriah [1988]. The *middle tunnel* of $K_{p,q}$ is represented by an arc in T that meets $K_{p,q}$ only in its endpoints. The *upper tunnel* of $K_{p,q}$ is represented by an arc α properly imbedded in W , such that the circle which is the union of α with one of the two arcs of $K_{p,q}$ with endpoints equal to the endpoints of α is a deformation retract of W . The *lower tunnel* is like the upper tunnel, but interchanging the roles of $V \cup T \times I$ and W . For some choices of p and q , some of these tunnels are equivalent.

A braid description for torus knots was obtained by A. Cattabriga and M. Mulazzani [Cattabriga and Mulazzani 2005, Section 4]. Here we will use a similar description due to A. Seo [2008]. Fix (p, q) relatively prime, and suppose for now that $p, q \geq 2$. In \mathbb{R}^2 we construct a polygonal path $P_{p,q}$ from $(0, 0)$ to (p, q) , as indicated in Figure 21 for the cases when (p, q) is $(3, 7)$ and $(7, 3)$, as follows: Regard \mathbb{R}^2 as made up of squares with side length 1, whose corners have integer coordinates. Consider the rectangle R with corners $(0, 0)$ and (p, q) , and let S be the union of the squares in \mathbb{R}^2 whose bottom sides contain no points above the line containing $(0, 0)$ and (p, q) . Then $P_{p,q}$ is $R \cap \partial S$.

Explicitly, for $0 \leq k \leq q$ put $p_k = \lceil kp/q \rceil$. The points (p_k, k) are indicated in Figure 21. The intersection point of the diagonal of R with the line $y = k$ has x -coordinate kp/q , so $\lceil kp/q \rceil$ is the x -coordinate of the first integral lattice point on $y = k$ that lies on or to the right of this intersection point. The path $P_{p,q}$ is the union for $1 \leq i \leq q$ of the segments (some of which may have length 0) from $(p_{i-1}, i-1)$ to (p_{i-1}, i) and from (p_{i-1}, i) to (p_i, i) .

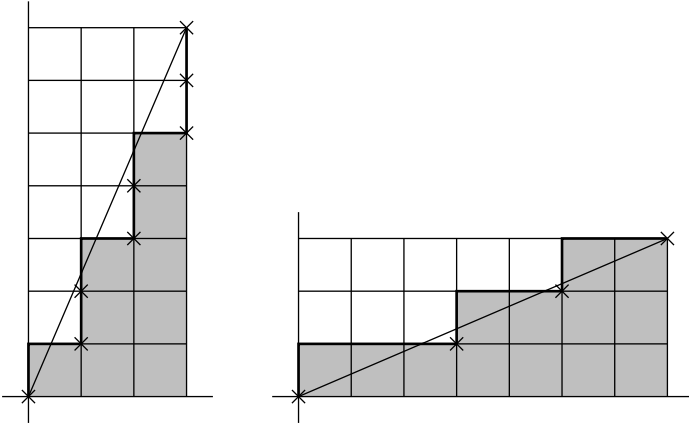


Figure 21. The points (p_k, k) for $0 \leq k \leq q$ for the cases $(p, q) = (3, 7)$ and $(p, q) = (7, 3)$.

We will now use $P_{p,q}$ to obtain a braid description of $K_{p,q}$. As usual, the braid portion will start in T . Referring again to [Figure 21](#), we may assume that the plane picture is drawn so that the lifts of the fixed arc α in T from the black point to the white point are short straight line segments positioned so that each meets only the translate of the diagonal of R that contains its lower left point (that is, its black point), and apart from that point lies below that translate.

Consider the braid β with the following description. As we descend in $T \times I$, the T -coordinate of the white point stays fixed, while the T -coordinate of the black point moves *backward* along the (p, q) -curve which is the image of the diagonal of the rectangle (that is, the lift to \mathbb{R}^2 of its path in T starting (p, q) travels along the diagonal of R to $(0, 0)$). The choice of the backward direction is not essential, but leads to a simpler calculation. Since each lift of α lie below the translate of the diagonal that it meets, the diagonal of R is isotopic, not crossing any lift of α and in particular not crossing any lift of the white point, to $P_{p,q}$. This implies that β is represented by the braid word whose letters correspond to the horizontal and vertical steps along $P_{p,q}$ (starting from the upper right), with each downward step being δ_m and each leftward step being δ_ℓ^{-1} . This word is

$$\omega_{(p,q)} = \delta_\ell^{p_{q-1}-p_q} \delta_m \cdots \delta_\ell^{p_0-p_1} \delta_m.$$

Similar considerations give a braid description for the case when $p > 0$ and $q < 0$. For $0 \leq k \leq p$ put $q_k = \lceil kq/p \rceil$. The braid is then

$$\omega_{(p,q)} = \prod_{k=0}^{p-1} \delta_\ell \delta_m^{q_k - q_{k+1}}.$$

Assuming as before that $p, q \geq 2$, we now use $\omega_{(p,q)}$ to compute the slope coefficients of the upper tunnel of $K_{p,q}$. We have

$$\begin{aligned}\omega_{(p,q)} &\sim \delta_m \delta_\ell^{p_{q-2}-p_{q-1}} \cdots \delta_m \delta_\ell^{p_1-p_2} \delta_m \delta_\ell^{p_0-p_1} \\ &= \delta_m \sigma \sigma^{-1} \delta_\ell^{p_{q-2}-p_{q-1}} \cdots \delta_m \sigma \sigma^{-1} \delta_\ell^{p_1-p_2} \delta_m \sigma \sigma^{-1} \delta_\ell^{p_0-p_1}.\end{aligned}$$

Putting $\omega_j = \delta_m \delta_\ell^{p_{j-1}-p_j} \cdots \delta_m \delta_\ell^{p_1-p_2} \delta_m \delta_\ell^{-p_1}$, we have

$$t(\omega_j) = (p_j - p_{j-1}) + \cdots + (p_2 - p_1) + (p_1 - p_0) = p_j - p_0 = p_j.$$

Now, working from the right, [Theorem 9.3](#) finds the cabling slope sequence for the upper tunnel:

$$\begin{aligned}[2(p_1 - p_0), -1] &= 2p_1 - 1 \\ [2t(\omega_1) + 2(p_2 - p_1), -1] &= 2p_2 - 1 \\ &\dots \\ [2t(\omega_{q-2}) + 2(p_{q-1} - p_{q-2}), -1] &= 2p_{q-1} - 1\end{aligned}$$

These give the trivial knot as long as $p_j \leq 1$, so we have reproved one of the main results from [\[Cho and McCullough 2009b\]](#):

Theorem 11.1. *Let p and q be relatively prime integers, both greater than 1. For $1 \leq k \leq q$, put $p_k = \lceil kp/q \rceil$, and let $k_0 = \min\{k \mid p_k > 1\}$. Then the upper tunnel of $K_{p,q}$ is produced by $q - k_0$ cabling constructions, whose slopes are*

$$[1/(2p_{k_0} - 1)], 2p_{k_0+1} - 1, \dots, 2p_{q-1} - 1.$$

Of course if $p, q < 0$, then $K_{p,q} = K_{-p,-q}$. When $pq < 0$, there is an orientation-reversing equivalence from $K_{p,q}$ to $K_{p,-q}$ which takes upper tunnel to upper tunnel, so the slopes are just the negatives of those given in [Theorem 11.1](#) for $K_{|p|,|q|}$. The lower tunnel of $K_{p,q}$ is equivalent to the upper tunnel of $K_{q,p}$, so [Theorem 11.1](#) also finds the slope sequences of the lower tunnels.

12. Toroidal (1, 1)-positions

As usual, we fix a decomposition $S^3 = V \cup T \times I \cup W$, with $T = T \times \{0\} = \partial W$ the standard torus in S^3 . A knot is said to be in a *toroidal* position if it is contained in $T \times I$ and both of the coordinate projections from $S^1 \times S^1 \times I$ to S^1 restrict to immersions on the knot. That is, when traveling along the knot, neither of the S^1 -coordinates ever reverses direction.

Theorem 12.1. *A simple or semisimple tunnel is the upper or lower tunnel of a toroidal (1, 1)-position if and only if its sequence of slope coefficients is of the*

form

$$[1/n_0], n_1, \dots, n_k$$

with the n_i , $1 \leq i \leq k$, either a nondecreasing sequence of positive odd integers or a nonincreasing sequence of negative odd integers.

Before proving [Theorem 12.1](#), we will use it to find the toroidal 2-bridge knots.

Corollary 12.2. *A 2-bridge knot K admits a toroidal $(1, 1)$ -position if and only if it satisfies one of the following equivalent conditions:*

- (i) *For some $n > 0$, its upper simple and upper semisimple tunnels have respective slope sequences either $[1/(2n + 1)]$ and $[1/3], 3, 3, \dots, 3$, or $[2n/(2n + 1)]$ and $[2/3], -3, -3, \dots, -3$, where the latter sequences in each case have length n .*
- (ii) *Its classifying invariants are $b/a = b'/a = 1/(2n + 1)$.*
- (iii) *It is a torus knot, in fact a $(2n + 1, \pm 2)$ -torus knot for some $n \neq 0$.*

Proof. Examining [Proposition 10.4](#), we find that the only 2-bridge knots whose upper semisimple tunnels have slope sequences satisfying the condition of [Theorem 12.1](#) are those whose rational invariants are given by the continued fractions

$$[-2, 2, -2, 2, \dots, -2, 2] \quad \text{and} \quad [2, -2, 2, -2, \dots, 2, -2],$$

which give the slope sequences in (i) and correspond to the invariants in (ii). Using [Theorem 11.1](#), these are exactly the torus knots listed in (iii). \square

We note that the 2-bridge knots in [Corollary 12.2](#) have only one $(1, 1)$ -position, so no two-bridge knot with two $(1, 1)$ -positions is toroidal.

Proof of [Theorem 12.1](#). A toroidal $(1, 1)$ -position is described by a braid of the form $\delta_m^{a_1} \delta_\ell^{b_1} \dots \delta_m^{a_n} \delta_\ell^{b_n}$ where the a_i all have the same sign and the same is true of the b_i 's. If the a_i are all negative, apply an orientation-reversing equivalence that reverses the orientation on the S^1 -factor corresponding to δ_m so that the a_i are all positive. Since this negates all the cabling slopes, it will not affect whether the slopes satisfy the conclusion of the theorem.

To compute the cabling slopes, it is convenient to allow some $b_j = 0$, and rewrite the braid as

$$\delta_m \delta_\ell^{b_0} \dots \delta_m \delta_\ell^{b_k} \sim \delta_m \sigma \sigma^{-1} \delta_\ell^{b_0} \dots \delta_m \sigma \sigma^{-1} \delta_\ell^{b_k}.$$

Using [Theorem 9.3](#) to read off the cabling slopes, working from the right, we obtain continued fractions

$$[-2b_k, -1], [-2(b_{k-1} + b_k), -1], \dots, [-2(b_0 + \dots + b_k), -1]$$

and the slope invariants are as claimed.

Conversely, given the sequence n_0, \dots, n_k , put $m_j = -(n_j + 1)/2$ and let K be in the $(1, 1)$ -position with braid description

$$\delta_m \delta_\ell^{m_k - m_{k-1}} \delta_m \delta_\ell^{m_{k-1} - m_{k-2}} \dots \delta_m \delta_\ell^{m_1 - m_0} \delta_m \delta_\ell^{m_0}.$$

Calculation as above finds the slope coefficients of the upper tunnel to be $[1/n_0], n_1, \dots, n_k$. \square

13. Algorithmic computation of braid descriptions

Using Theorems 8.1 and 9.3, it is not difficult to obtain a braid description for a $(1, 1)$ -position of a knot from the slope sequence $[m_0], m_1, \dots, m_d$ of its upper $(1, 1)$ -tunnel:

- (i) Assuming that m_0 is selected so that $0 < m_0 < 1$, write $1/m_0$ as a continued fraction of the form $[2a_1, b_1, 2a_2, \dots, 2a_n, b_n]$. Put

$$\omega_0 = \delta_m \sigma \cdot \sigma^{b_n} \delta_\ell^{-a_n} \dots \sigma^{b_1} \delta_\ell^{-a_1}.$$

If we start with the trivial knot in braid position with braid description 1, by Theorems 8.1 and 9.3 a cabling construction of slope $[2a_1, b_1, 2a_2, \dots, 2a_n, b_n]$ (on the upper tunnel) produces the knot with braid description ω_0 . Since this is the initial cabling, its simple slope is $[1/[2a_1, b_1, 2a_2, \dots, 2a_n, b_n]] = [m_0]$.

- (ii) Write m_1 in the form $[2a_1, b_1, \dots, 2a_n, b_n]$, and put

$$\omega_1 = \delta_m \sigma \cdot \sigma^{b_n} \delta_\ell^{-a_n} \dots \sigma^{b_1} \delta_\ell^{-a_1} \cdot \delta_\ell^{t(\omega_0)}.$$

By Theorems 8.1 and 9.3, a cabling of slope

$$m_1 = [2t(\omega_0) + 2(a_1 - t(\omega_0)), b_1, 2a_2, \dots, b_n]$$

now produces a knot in $(1, 1)$ -position with braid description $\omega_1 \omega_0$.

- (iii) Write m_2 as $[2a_1, b_1, \dots, 2a_n, b_n]$, put $\omega_2 = \delta_m \sigma \cdot \sigma^{b_n} \delta_\ell^{-a_n} \dots \sigma^{b_n} \delta_\ell^{-a_1} \cdot \delta_\ell^{t(\omega_1 \omega_0)}$, and so on.

- (iv) Put $w = \omega_d \dots \omega_1 \omega_0$.

14. Algorithmic computation of slope invariants

In this section we develop an effective algorithm for computing the slope invariants of an upper or lower tunnel of a $(1, 1)$ -position given by a braid description. We will only concern ourselves with the upper tunnel, since the lower tunnel is the upper tunnel of the knot described by the reverse braid.

The basic approach is obvious from the various examples that we have seen computed; the main difficulties will arise in the technical matter of dealing with anomalous infinite slopes.

We start by writing the given braid description in the form

$$W_0(\delta_\ell, \sigma) \omega W_1(\delta_m, \sigma),$$

where ω starts with $\delta_m^{\pm 1}$ and ends with $\delta_\ell^{\pm 1}$, and $W_0(\delta_\ell, \sigma)$ and $W_1(\delta_m, \sigma)$ are words in the indicated letters. Replacing each appearance of δ_m^{-1} in ω with $\sigma \delta_m \sigma$, we can write

$$\omega \sim \delta_m \sigma \cdot \omega_d(\delta_\ell, \sigma) \cdot \delta_m \sigma \cdot \omega_{d-1}(\delta_\ell, \sigma) \cdots \delta_m \sigma \cdot \omega_0(\delta_\ell, \sigma)$$

where each $\omega_i(\delta_\ell, \sigma)$ lies in $\langle \delta_\ell, \sigma \rangle$.

According to [Theorem 8.1](#), the $(1, 1)$ -position described by ω is obtained starting from the trivial position (with braid description 1 and upper tunnel in standard position) by a sequence of $d + 1$ cabling constructions with slopes given as in [Theorem 9.3](#). It may happen, however, that some have infinite slope (hence, strictly speaking, are not genuine cabling constructions). This occurs exactly when the slope given by [Theorem 9.3](#) would be infinite — for instance, when $\omega_i(\delta_\ell, \sigma) = \delta_\ell^k$ for some integer k , since then the slope is of the form $[2t - 2k, 0] = \infty$.

To understand when the cabling produced by $\delta_m \sigma \cdot \omega_i(\delta_\ell, \sigma)$ has infinite slope, we will need a description of the subgroup $\langle \delta_\ell, \sigma \rangle$ of \mathcal{B} . The Reidemeister–Schreier algorithm does not seem to be effective in this case, but there is an easy argument giving a presentation for this subgroup:

Lemma 14.1. *The subgroup $\langle \delta_\ell, \sigma \rangle$ of \mathcal{B} has presentation*

$$\langle \delta_\ell, \sigma \mid (\delta_\ell \sigma)^2 = 1 \rangle.$$

Proof. Let $\overline{\mathcal{B}}$ be the quotient of \mathcal{B} obtained by adding the relation $\delta_m^2 = 1$. It has presentation

$$\overline{\mathcal{B}} = \langle \overline{\delta}_m, \overline{\delta}_\ell, \overline{\sigma} \mid (\overline{\delta}_\ell \overline{\sigma})^2 = 1, \overline{\delta}_m \overline{\sigma} \overline{\delta}_m^{-1} = \overline{\sigma}^{-1}, \overline{\delta}_m \overline{\delta}_\ell \overline{\delta}_m^{-1} = \overline{\sigma}^2 \overline{\delta}_\ell, \overline{\delta}_m^2 = 1 \rangle$$

which we may regard as a semidirect product

$$\langle \overline{\delta}_\ell, \overline{\sigma} \mid (\overline{\delta}_\ell \overline{\sigma})^2 = 1 \rangle \rtimes \langle \overline{\delta}_m \mid \overline{\delta}_m^2 = 1 \rangle.$$

There is an obvious homomorphism $\langle \delta_\ell, \sigma \mid (\delta_\ell \sigma)^2 = 1 \rangle \rightarrow \mathcal{B}$, and the composition $\langle \delta_\ell, \sigma \mid (\delta_\ell \sigma)^2 = 1 \rangle \rightarrow \mathcal{B} \rightarrow \overline{\mathcal{B}}$ carries $\langle \delta_\ell, \sigma \mid (\delta_\ell \sigma)^2 = 1 \rangle$ isomorphically to $\langle \overline{\delta}_\ell, \overline{\sigma} \mid (\overline{\delta}_\ell \overline{\sigma})^2 = 1 \rangle$. The lemma follows. \square

By [Lemma 14.1](#), $\langle \delta_\ell, \sigma \rangle$ is a free product of the form $C_2 * C_\infty$, where C_2 is generated by $\delta_\ell \sigma$ and C_∞ is generated by σ . Recall the elementary matrices $U = \begin{bmatrix} 1 & 1 \\ 0 & 1 \end{bmatrix}$ and $L = \begin{bmatrix} 1 & 0 \\ 1 & 1 \end{bmatrix}$ from [Section 7](#).

Lemma 14.2. *The subgroup $\langle L^2, U \rangle$ of $\mathrm{PSL}(2, \mathbb{Z})$ is given by the presentation $\langle L^2, U \mid (L^{-2}U)^2 = I \rangle$. Consequently, sending δ_ℓ to L^{-2} and σ to U defines an isomorphism from the subgroup $\langle \delta_\ell, \sigma \rangle$ of \mathcal{B} to $\langle L^2, U \rangle$.*

Proof. We use the homomorphism $\mathrm{PSL}(2, \mathbb{Z}) \rightarrow \mathrm{PSL}(2, \mathbb{Z}/2) = \mathrm{SL}(2, \mathbb{Z}/2)$, where the latter is isomorphic to the permutation group on three letters. One can check that $\langle L^2, U \rangle$ consists exactly of the elements of the form $\begin{bmatrix} a & b \\ 2c & d \end{bmatrix}$, so $\langle L^2, U \rangle$ is the inverse image of the subgroup $\langle I, \begin{bmatrix} 1 & 1 \\ 0 & 1 \end{bmatrix} \rangle$ of $\mathrm{PSL}(2, \mathbb{Z}/2)$. Therefore $\langle L^2, U \rangle$ has index 3 in $\mathrm{PSL}(2, \mathbb{Z})$. Note also that this shows that every element of $\langle L^2, U \rangle$ has even trace, and hence is not of order 3.

It is well-known that $\mathrm{PSL}(2, \mathbb{Z}) \cong C_2 * C_3$. Since $\langle L^2, U \rangle$ is a two-generator subgroup, it is a free product of two cyclic subgroups. It contains the involution $L^{-2}U$, and no elements of order 3, so is isomorphic to either $C_2 * C_\infty$ or $C_2 * C_2$. The latter is impossible since $C_2 * C_2$ contains an infinite cyclic subgroup of index 2, which would have index 6 in $\mathrm{PSL}(2, \mathbb{Z})$. Every element of order 2 in $C_2 * C_\infty$ is conjugate to the generator of C_2 , so as generators of the free factors we may choose the involution $L^{-2}U$ and the infinite order element U . The lemma follows, making use of [Lemma 14.1](#). \square

Lemma 14.3. *Let $S \subset \mathbb{Q} \cup \{\infty\}$ consist of the a/b with a odd. Sending*

$$\sigma^{b_n} \delta_\ell^{-a_n} \dots \sigma^{b_1} \delta_\ell^{-a_1}$$

to the element of $\mathbb{Q} \cup \{\infty\}$ given by the continued fraction $[2a_1, b_1, \dots, 2a_n, b_n]$ induces a bijection from the set of right cosets $\langle \delta_\ell \rangle \backslash \langle \delta_\ell, \sigma \rangle$ to S .

Proof. Regard the elements a/b of $\mathbb{Q} \cup \{\infty\}$ as row vectors $[a \ b]$ (with $[a \ b]$ equivalent to $[an \ bn]$ for $n \neq 0$). Define an action of $\langle \delta_\ell, \sigma \rangle$ on the right on S by

$$[a \ b] \delta_\ell = [a \ b] L^{-2} \quad \text{and} \quad [a \ b] \sigma = [a \ b] U,$$

where U and L are the upper and lower elementary matrices as in [Section 7](#). Since $L^{-2}UL^{-2}U = -I$ acts trivially on elements of $\mathbb{Q} \cup \{\infty\}$, [Lemma 14.2](#) shows that this is well-defined. We have

$$[a \ b] \sigma^{b_n} \delta_\ell^{-a_n} \dots \sigma^{b_1} \delta_\ell^{-a_1} = [a \ b] U^{b_n} L^{2a_n} \dots U^{b_1} L^{2a_1}$$

and taking the transpose gives

$$U^{2a_1} L^{b_1} \dots U^{2a_n} L^{b_n} \begin{bmatrix} a \\ b \end{bmatrix} = \begin{bmatrix} q & s \\ p & r \end{bmatrix} \begin{bmatrix} a \\ b \end{bmatrix},$$

where, according to [Lemma 14.3](#) of [\[Cho and McCullough 2009a\]](#), q/p has continued fraction expansion $[2a_1, b_1, \dots, 2a_n, b_n]$. Every a/b with a odd can be written as a continued fraction of the form $[2a_1, b_1, \dots, 2a_n, b_n]$, by [Lemma 14.2](#) of the same reference, so $[1 \ 0] \sigma^{b_n} \delta_\ell^{-a_n} \dots \sigma^{b_1} \delta_\ell^{-a_1} = [2a_1, b_1, \dots, 2a_n, b_n]$ and therefore the action is transitive on S . One can check easily that the stabilizer of $[1 \ 0]$ under the right action of $\mathrm{PSL}(2, \mathbb{Z})$ is the subgroup generated by L . Using [Lemma 14.2](#), the stabilizer of $1/0 \in S$ under the action of $\langle \delta_\ell, \sigma \rangle$ is $\langle \delta_\ell \rangle$. \square

Proposition 14.4. *Suppose the cabling produced by the segment $\delta_m \sigma \cdot \omega_i(\delta_\ell, \sigma)$ of the braid description ω has infinite slope. Then*

$$\omega_i(\delta_\ell, \sigma) = \delta_\ell^{-t(\omega_i(\delta_\ell, \sigma))}$$

in $\langle \delta_\ell, \sigma \rangle$.

Proof. Write $\omega_i(\delta_\ell, \sigma) = \sigma^{b_n} \delta_\ell^{-a_n} \dots \sigma^{b_1} \delta_\ell^{-a_1}$. By [Theorem 9.3](#), the cabling produced by $\delta_m \sigma \cdot \omega_i(\delta_\ell, \sigma)$ has slope $[2t + 2a_1, b_1, \dots, 2a_n, b_n]$, where t is the algebraic winding number of the portion of ω that follows $\omega_i(\delta_\ell, \sigma)$. By [Lemma 14.3](#), this is infinite exactly when $\sigma^{b_n} \delta_\ell^{-a_n} \dots \sigma^{b_1} \delta_\ell^{-a_1}$ is equal in $\langle \delta_\ell, \sigma \rangle$ to some power δ_ℓ^k . Since inserting or deleting the word $\delta_\ell \sigma \delta_\ell \sigma$ does not change the winding number of a braid, we have $t(\omega_i(\delta_\ell, \sigma)) = t(\delta_\ell^k) = -k$ and the lemma follows. \square

We can now give the algorithm. Suppose that in the braid description $\delta_m \sigma \cdot \omega_d(\delta_\ell, \sigma) \cdot \delta_m \sigma \cdot \omega_{d-1}(\delta_\ell, \sigma) \dots \delta_m \sigma \cdot \omega_0(\delta_\ell, \sigma)$, the portion $\delta_m \sigma \cdot \omega_i(\delta_\ell, \sigma)$ produces a cabling of infinite slope. If $i \neq 0, d$, we have

$$\begin{aligned} & \dots \omega_{i+1}(\delta_\ell, \sigma) \delta_m \sigma \omega_i(\delta_\ell, \sigma) \delta_m \sigma \omega_{i-1}(\delta_\ell, \sigma) \delta_m \sigma \dots \\ &= \dots \omega_{i+1}(\delta_\ell, \sigma) \delta_m \sigma \delta_\ell^{-t(\omega_i(\delta_\ell, \sigma))} \delta_m \sigma \omega_{i-1}(\delta_\ell, \sigma) \delta_m \sigma \dots \\ &= \dots \omega_{i+1}(\delta_\ell, \sigma) \delta_\ell^{t(\omega_i(\delta_\ell, \sigma))} \delta_m \sigma \delta_m \sigma \omega_{i-1}(\delta_\ell, \sigma) \delta_m \sigma \dots \\ &= \dots \omega_{i+1}(\delta_\ell, \sigma) \delta_\ell^{t(\omega_i(\delta_\ell, \sigma))} \omega_{i-1}(\delta_\ell, \sigma) \delta_m \sigma \dots \end{aligned}$$

with d decreased by 2. In going from the second line to the third, we used the fact that

$$\delta_m \sigma \delta_\ell = \delta_m \delta_\ell^{-1} \sigma^{-2} \sigma = \delta_m \delta_\ell^{-1} (\delta_\ell \delta_m^{-1} \delta_\ell^{-1} \delta_m) \sigma = \delta_\ell^{-1} \delta_m \sigma.$$

In the special case when $i = d$, this looks like

$$\begin{aligned} & \delta_m \sigma \delta_\ell^{-t(\omega_d(\delta_\ell, \sigma))} \delta_m \sigma \omega_{d-1}(\delta_\ell, \sigma) \delta_{d-2} \sigma \omega_3(\delta_\ell, \sigma) \dots \\ &= \delta_\ell^{t(\omega_d(\delta_\ell, \sigma))} \delta_m \sigma \delta_m \sigma \omega_{d-1}(\delta_\ell, \sigma) \delta_{d-2} \sigma \omega_3(\delta_\ell, \sigma) \dots \\ &= \delta_\ell^{t(\omega_d(\delta_\ell, \sigma))} \omega_{d-1}(\delta_\ell, \sigma) \delta_m \sigma \omega_{d-2}(\delta_\ell, \sigma) \dots \\ &\sim \delta_m \sigma \omega_{d-2}(\delta_\ell, \sigma) \end{aligned}$$

with d decreased by 2.

In the special case when $i = 0$, we have

$$\begin{aligned} & \dots \omega_1(\delta_\ell, \sigma) \delta_m \sigma \omega_0(\delta_\ell, \sigma) \\ &= \dots \omega_1(\delta_\ell, \sigma) \delta_m \sigma \delta_\ell^{-t(\omega_0(\delta_\ell, \sigma))} \\ &= \dots \omega_1(\delta_\ell, \sigma) \delta_\ell^{t(\omega_0(\delta_\ell, \sigma))} \delta_m \sigma \\ &\sim \dots \omega_1(\delta_\ell, \sigma) \delta_\ell^{t(\omega_0(\delta_\ell, \sigma))} \end{aligned}$$

with d decreased by 1.

We repeat these until there are no cablings of infinite slope. The cabling slopes can then be read off from the new $\omega_i(\delta_\ell, \sigma)$, starting from the rightmost. Some of the initial cablings may have integral *simple* slope, which occurs when their ordinary slope is of the form $1/k$. The first slope invariant is obtained by inverting the first slope not of the form $1/k$ (and regarding the result as an element of \mathbb{Q}/\mathbb{Z}). In terms of the algebraic manipulations we have been doing, what is happening is this: When the slope associated to $\omega_0(\delta_\ell, \sigma)$ is some $1/k$, its continued fraction has value equal to that of the continued fraction $[0, k]$. [Lemma 14.3](#) shows that $\omega_0(\delta_\ell, \sigma)$ is equal to $\delta_\ell^{-t(\omega_0(\delta_\ell, \sigma))} \sigma^k$. So we have

$$\begin{aligned} & \cdots \omega_1(\delta_\ell, \sigma) \delta_m \sigma \omega_0(\delta_\ell, \sigma) \\ &= \cdots \omega_1(\delta_\ell, \sigma) \delta_m \sigma \delta_\ell^{-t(\omega_0(\delta_\ell, \sigma))} \sigma^k \\ &= \cdots \omega_1(\delta_\ell, \sigma) \delta_\ell^{t(\omega_0(\delta_\ell, \sigma))} \delta_m \sigma \sigma^k \\ &\sim \cdots \omega_1(\delta_\ell, \sigma) \delta_\ell^{t(\omega_0(\delta_\ell, \sigma))} \end{aligned}$$

with d decreased by 1.

15. Computations

We have implemented the algorithms of Sections 13 and 14 in Python; the program is available in the [Electronic Supplement](#) or at [\[Cho and McCullough 2010b\]](#). In this section, we give some sample calculations.

Using the algorithm of [Section 14](#), slopes of the upper tunnel or lower tunnel are computed from a braid description. For example, the braid $\delta_m^3 \sigma^{-2} \delta_\ell^3 \sigma^{-4} \delta_m^{-1} \sigma^{-4} \delta_\ell^3$ gives

```
Semisimple> upperSlopes( 'm 3 s -2 l 3 s -4 m -1 s -4 l 3' )
[ 21/25 ], 341/60, -13, -13
```

To compute the lower slopes, the script just finds the reverse braid and applies `upperSlopes`:

```
Semisimple> lowerSlopes( 'm 3 s -2 l 3 s -4 m -1 s -4 l 3' )
[ 16/19 ], -7, -7, -195/31, -5, -5
```

Using the method of [Section 13](#), a braid describing the $(1, 1)$ -position can be recovered from the upper tunnel slope sequence. In the next example, the slope sequence $[21/25], 341/60, -13, -13$ is represented as the input list

$$[21, 25, 341, 60, -13, 1, -13, 1] :$$

```
Semisimple> print braidWord( [21,25,341,60,-13,1,-13,1] )
m 3 s -3 m -1 l -2 m 1 l -1 s -4 m 1 s -4 m -1 l -2 m 1 l -1
```

which checks:

```
Semisimple> upperSlopes( 'm 3 s -3 m -1 l -2 m 1 l -1 s -4
m 1 s -4 m -1 l -2 m 1 l -1' )
[ 21/25 ], 341/60, -13, -13
```

To compute the slopes of one tunnel associated to a $(1, 1)$ -position from the slopes of the other, the script generates a braid describing an upper tunnel which has those slopes, then find the slope sequence of the lower tunnel:

```
Semisimple> dualSlopes([21,25,341,60,-13,1,-13,1])
[ 16/19 ], -7, -7, -195/31, -5, -5
Semisimple> dualSlopes([16,19,-7,1,-7,1,-195,31,-5,1,-5,1])
[ 21/25 ], 341/60, -13, -13
```

Functions are also included which calculate slope sequences for semisimple tunnels of 2-bridge and torus knots. For example, for 2-bridge knots we have

```
Semisimple> twoBridge( 413, 227 )
Upper simple tunnel: [ 131/413 ]
Upper semisimple tunnel: [ 1/3 ], 15/7, 9/5
Lower simple tunnel: [ 227/413 ]
Lower semisimple tunnel: [ 2/5 ], -1, -3/2, 1, 1, 1, 3
Semisimple> print upperSemisimpleBraidWord( 413, 227 )
m -1 s -6 m -1 s 6 m -1 s 1 l -1
Semisimple> print lowerSimpleBraidWord( 413, 227 )
m -1 s 1 l -1 s 6 l -1 s -6 l -1
```

For torus knots, we have:

```
Semisimple> torusUpperSlopes( 13, 5 )
[ 1/5 ], 11, 15, 21
Semisimple> torusLowerSlopes( 13, 5 )
[ 1/3 ], 3, 3, 5, 5, 7, 7, 7, 9, 9
Semisimple> print fullTorusBraidWord( 13, 5 )
l -2 m 1 l -3 m 1 l -2 m 1 l -3 m 1 l -3 m 1
```

Theorem 10.5 allows us to test whether a slope sequence belongs to some 2-bridge knot tunnel:

```
Semisimple> find2BridgeKnot( [ 1, 3, 15, 7, 9, 5 ] )
The tunnel is the upper semisimple tunnel of  $K(413, 227)$ , or
equivalently the lower semisimple tunnel of  $K(413, 131)$ .
Semisimple> find2BridgeKnot( [ 1, 3, 15, 8, -9, 5 ] )
The tunnel is the upper semisimple tunnel of  $K(493, 222)$ , or
equivalently the lower semisimple tunnel of  $K(493, 171)$ .
```

```
Semisimple> find2BridgeKnot( [ 1, 3, 15, 11, 9, 5 ] )
Slopes other than first must be of the form  $2 + 1/k$  or  $2 - 1/k$ .

Semisimple> find2BridgeKnot( [ 1, 3, 15, 8, 9, 5 ] )
The  $i$ th and  $(i+1)$ st slopes must have opposite signs
when  $k \text{ sub } i$  is even.

Semisimple> find2BridgeKnot( [ 1, 3, -15, 8, 9, 5 ] )
 $m_1$  must be positive or negative according as  $n_0$  is odd or even.
```

References

- [Akbas 2008] E. Akbas, “A presentation for the automorphisms of the 3-sphere that preserve a genus two Heegaard splitting”, *Pacific J. Math.* **236**:2 (2008), 201–222. [MR 2009d:57029](#) [Zbl 1157.57002](#)
- [Birman 1969] J. S. Birman, “On braid groups”, *Comm. Pure Appl. Math.* **22** (1969), 41–72. [MR 38 #2764](#) [Zbl 0157.30904](#)
- [Boileau et al. 1988] M. Boileau, M. Rost, and H. Zieschang, “On Heegaard decompositions of torus knot exteriors and related Seifert fibre spaces”, *Math. Ann.* **279**:3 (1988), 553–581. [MR 89a:57013](#) [Zbl 0616.57008](#)
- [Cattabriga and Mulazzani 2004] A. Cattabriga and M. Mulazzani, “(1, 1)-knots via the mapping class group of the twice punctured torus”, *Adv. Geom.* **4**:2 (2004), 263–277. [MR 2005e:57013](#) [Zbl 1079.57003](#)
- [Cattabriga and Mulazzani 2005] A. Cattabriga and M. Mulazzani, “Representations of (1, 1)-knots”, *Fund. Math.* **188** (2005), 45–57. [MR 2006j:57027](#) [Zbl 1089.57005](#)
- [Cho 2008] S. Cho, “Homeomorphisms of the 3-sphere that preserve a Heegaard splitting of genus two”, *Proc. Amer. Math. Soc.* **136**:3 (2008), 1113–1123. [MR 2009c:57029](#) [Zbl 1149.57025](#)
- [Cho and McCullough 2009a] S. Cho and D. McCullough, “The tree of knot tunnels”, *Geom. Topol.* **13**:2 (2009), 769–815. [MR 2010j:57005](#) [Zbl 1191.57005](#)
- [Cho and McCullough 2009b] S. Cho and D. McCullough, “Cabling sequences of tunnels of torus knots”, *Algebr. Geom. Topol.* **9**:1 (2009), 1–20. [MR 2009i:57011](#) [Zbl 1170.57005](#)
- [Cho and McCullough 2010a] S. Cho and D. McCullough, “Constructing knot tunnels using giant steps”, *Proc. Amer. Math. Soc.* **138**:1 (2010), 375–384. [MR 2011b:57004](#) [Zbl 1192.57004](#)
- [Cho and McCullough 2010b] S. Cho and D. McCullough, [Software for “Semisimple tunnels”](#), 2010, available at <http://www2.math.ou.edu/~dmccullough/research/python/semisimple.py>.
- [Cho and McCullough 2011] S. Cho and D. McCullough, “Tunnel leveling, depth, and bridge numbers”, *Trans. Amer. Math. Soc.* **363**:1 (2011), 259–280. [MR 2012d:57004](#) [Zbl 1210.57004](#)
- [Ishihara 2011] K. Ishihara, “An algorithm for finding parameters of tunnels”, *Algebr. Geom. Topol.* **11**:4 (2011), 2167–2190. [MR 2826935](#) [Zbl 1232.57010](#)
- [Moriah 1988] Y. Moriah, “Heegaard splittings of Seifert fibered spaces”, *Invent. Math.* **91**:3 (1988), 465–481. [MR 89d:57010](#) [Zbl 0651.57012](#)
- [Morimoto and Sakuma 1991] K. Morimoto and M. Sakuma, “On unknotting tunnels for knots”, *Math. Ann.* **289**:1 (1991), 143–167. [MR 92e:57015](#) [Zbl 0697.57002](#)
- [Scharlemann 2004] M. Scharlemann, “Automorphisms of the 3-sphere that preserve a genus two Heegaard splitting”, *Bol. Soc. Mat. Mexicana* (3) **10**:Special Issue (2004), 503–514. [MR 2007c:57020](#) [Zbl 1095.57017](#) [arXiv math/0307231](#)

[Seo 2008] A. Seo, *Torus leveling of $(1, 1)$ -knots*, thesis, University of Oklahoma, 2008, available at <http://tinyurl.com/Seo-2008-thesis>. [MR 2711443](#)

[Takebayashi 2006] T. Takebayashi, “On the braid group of the torus T^2 ”, *JP J. Algebra Number Theory Appl.* **6:3** (2006), 585–595. [MR 2007i:20062](#) [Zbl 1120.20036](#)

Received July 28, 2011.

SANGBUM CHO
DEPARTMENT OF MATHEMATICS EDUCATION
HANYANG UNIVERSITY
SEOUL 133-791
SOUTH KOREA
scho@hanyang.ac.kr

DARRYL MCCULLOUGH
DEPARTMENT OF MATHEMATICS
UNIVERSITY OF OKLAHOMA
NORMAN, OK 73019-3103
UNITED STATES
dmccullough@math.ou.edu
www.math.ou.edu/~dmccullough/

PACIFIC JOURNAL OF MATHEMATICS

<http://pacificmath.org>

Founded in 1951 by

E. F. Beckenbach (1906–1982) and F. Wolf (1904–1989)

EDITORS

V. S. Varadarajan (Managing Editor)
Department of Mathematics
University of California
Los Angeles, CA 90095-1555
pacific@math.ucla.edu

Vyjayanthi Chari
Department of Mathematics
University of California
Riverside, CA 92521-0135
chari@math.ucr.edu

Darren Long
Department of Mathematics
University of California
Santa Barbara, CA 93106-3080
long@math.ucsb.edu

Sorin Popa
Department of Mathematics
University of California
Los Angeles, CA 90095-1555
popa@math.ucla.edu

Robert Finn
Department of Mathematics
Stanford University
Stanford, CA 94305-2125
finn@math.stanford.edu

Jiang-Hua Lu
Department of Mathematics
The University of Hong Kong
Pokfulam Rd., Hong Kong
jhlu@maths.hku.hk

Jie Qing
Department of Mathematics
University of California
Santa Cruz, CA 95064
qing@cats.ucsc.edu

Kefeng Liu
Department of Mathematics
University of California
Los Angeles, CA 90095-1555
liu@math.ucla.edu

Alexander Merkurjev
Department of Mathematics
University of California
Los Angeles, CA 90095-1555
merkurev@math.ucla.edu

Jonathan Rogawski
Department of Mathematics
University of California
Los Angeles, CA 90095-1555
jonr@math.ucla.edu

PRODUCTION

pacific@math.berkeley.edu

Silvio Levy, Scientific Editor

Mathew Cargo, Senior Production Editor

SUPPORTING INSTITUTIONS

ACADEMIA SINICA, TAIPEI
CALIFORNIA INST. OF TECHNOLOGY
INST. DE MATEMÁTICA PURA E APLICADA
KEIO UNIVERSITY
MATH. SCIENCES RESEARCH INSTITUTE
NEW MEXICO STATE UNIV.
OREGON STATE UNIV.

STANFORD UNIVERSITY
UNIV. OF BRITISH COLUMBIA
UNIV. OF CALIFORNIA, BERKELEY
UNIV. OF CALIFORNIA, DAVIS
UNIV. OF CALIFORNIA, LOS ANGELES
UNIV. OF CALIFORNIA, RIVERSIDE
UNIV. OF CALIFORNIA, SAN DIEGO
UNIV. OF CALIF., SANTA BARBARA

UNIV. OF CALIF., SANTA CRUZ
UNIV. OF MONTANA
UNIV. OF OREGON
UNIV. OF SOUTHERN CALIFORNIA
UNIV. OF UTAH
UNIV. OF WASHINGTON
WASHINGTON STATE UNIVERSITY

These supporting institutions contribute to the cost of publication of this Journal, but they are not owners or publishers and have no responsibility for its contents or policies.

See inside back cover or pacificmath.org for submission instructions.

The subscription price for 2012 is US \$420/year for the electronic version, and \$485/year for print and electronic. Subscriptions, requests for back issues from the last three years and changes of subscribers address should be sent to Pacific Journal of Mathematics, P.O. Box 4163, Berkeley, CA 94704-0163, U.S.A. Prior back issues are obtainable from Periodicals Service Company, 11 Main Street, Germantown, NY 12526-5635. The Pacific Journal of Mathematics is indexed by [Mathematical Reviews](#), [Zentralblatt MATH](#), [PASCAL CNRS Index](#), [Referativnyi Zhurnal](#), [Current Mathematical Publications](#) and the [Science Citation Index](#).

The Pacific Journal of Mathematics (ISSN 0030-8730) at the University of California, c/o Department of Mathematics, 969 Evans Hall, Berkeley, CA 94720-3840, is published monthly except July and August. Periodical rate postage paid at Berkeley, CA 94704, and additional mailing offices. POSTMASTER: send address changes to Pacific Journal of Mathematics, P.O. Box 4163, Berkeley, CA 94704-0163.

PJM peer review and production are managed by EditFLOW™ from Mathematical Sciences Publishers.

PUBLISHED BY PACIFIC JOURNAL OF MATHEMATICS

at the University of California, Berkeley 94720-3840

A NON-PROFIT CORPORATION

Typeset in L^AT_EX

Copyright ©2012 by Pacific Journal of Mathematics

PACIFIC JOURNAL OF MATHEMATICS

Volume 258 No. 1 July 2012

On the complexity of sails	1
LUKAS BRANTNER	
Construction of Lagrangian submanifolds in $\mathbb{C}\mathbb{P}^n$	31
QING CHEN, SEN HU and XIAOWEI XU	
Semisimple tunnels	51
SANGBUM CHO and DARRYL MCCULLOUGH	
Degenerate two-boundary centralizer algebras	91
ZAJJ DAUGHERTY	
Heegaard genera in congruence towers of hyperbolic 3-manifolds	143
BOGWANG JEON	
The Heisenberg ultrahyperbolic equation: The basic solutions as distributions	165
ANTHONY C. KABLE	
Rational Seifert surfaces in Seifert fibered spaces	199
JOAN E. LICATA and JOSHUA M. SABLOFF	
Delaunay cells for arrangements of flats in hyperbolic space	223
ANDREW PRZEWORSKI	